6-2021

Radar Network Synchronization and Imaging using Semiconductor Laser System

Meesha Gupta
Union College - Schenectady, NY

Radar Network Synchronization and Imaging using Semiconductor Laser System

By

Meesha Gupta

****

Submitted in partial fulfillment

of the requirements for

Honors in the Department of Electrical Engineering

UNION COLLEGE

June, 2021

Abstract

GUPTA, MEESHA Radar Network Synchronization and Imaging using Semiconductor Laser System. Department of Electrical Engineering, June 2021

ADVISOR: Chandra S. Pappu

The purpose of this project is to report the software implementation of radar network synchronization and imaging using a semiconductor laser system. We compare different radar configurations and methods to generate laser chaos.

The monostatic radar configuration has limited capabilities of detecting targets with low radar cross-sections[1]-[3]. This configuration is also vulnerable to intentional interference. In contrast, a radar network where multiple radar transceivers (nodes) are placed strategically can yield superior detection[1]-[3]. This radar network can also extract additional information about the target, such as its size and shape. However, synchronizing the nodes in the radar network poses a significant challenge. In this work, we utilize the self-synchronization property of chaos and propose that the semiconductor chaotic laser system can be used to synchronize all the nodes in the radar network. Through preliminary investigation, we show that the cross-correlation between the transmitter and synchronized radar node is of high quality with the main lobe width equivalent to a fraction of 1 nanosecond. Consequently, the range resolution of a few centimeters is achievable. Results of correlational analysis of our synchronized radar network are also shown. This analysis yielded sharp correlation peaks indicating the presence of multiple targets in close proximity.

Table of Contents

List of Figures

List of Tables

1. Introduction

1.1 Problem Statement

A wide bandwidth waveform transmission is necessary to achieve high-resolution imaging of radar targets. The problem with the current radar network is that several additional radiofrequency (RF) devices, such as voltage control oscillators and high bandwidth mixers, etc. are required[2]-[4]. This would create unwanted noise to perform the signal processing. Also, monostatic radar configurations are vulnerable to interference and jamming. Consequently, multi-static radar network configuration is gaining significant attention. A problem associated with this configuration is that the synchronization between each radar node is necessary to do the correlation analysis for detecting the targets. This is typically achieved using expensive hardware such as a global positioning system, crystal oscillator, etc. To counter this, we propose the use of semiconductor laser systems for radar network synchronization. These systems also generate wideband chaotic signals that oscillate at higher frequencies (in the order of a few GHz), which is necessary for high-resolution radar imaging.

In this project, we investigate the potentials of semiconductor chaotic waveforms for synchronizing the nodes of each radar network. Using correlation analysis, we also explore the resolution capabilities by considering the two closely spaced targets.

1.2 Motivation

In the past, various methods to synchronize a radar network have been proposed. Some of them are using synchronization clocks[1]-[3], oven-controlled crystal oscillators[11],

GPS systems[1], complex circuits[2], and additional expensive hardware at the receiver. Through our research, we will replace these types of equipment with a semiconductor laser system that can efficiently synchronize our radar network. This might filter out noise up to certain degree of freedom, and will help generate imagery of our targets without any interference.

Along with synchronization, we need to ensure that we use high-quality chaotic signals to help locate targets efficiently. Previously, Fan-Yi Lin and Jia-Ming Liu[4] have contrasted the quality of chaotic signals by using different semiconductor laser systems. Taking inspiration from their work, we will be presenting our testing results for different laser chaotic systems using metrics like range resolution, autocorrelation, the spectrum of the transmitted signal, correlational analysis, and two-point target simulation. This analysis will help us choose the best semiconductor laser system to generate wideband chaotic signals for high-resolution radar imaging.

1.3 Goals

Our idea is to work on simulations of multi-static radar network configuration. In this setup, each transmitter transmits a chaotic waveform that is statistically independent of other transmitted waveforms. Similarly, each receiving antenna receives an echo reflected by the target [9]. The received signal tends to have a high correlation only when the received waveform is a delayed and Doppler-shifted replica of the transmitted waveform[2].

In this research, we will show that the radar networks with multiple transmitter and receiver nodes can be synchronized easily using laser chaos. We will examine the quality

of signals generated by semiconductor laser systems using the metrics stated in section 1.2. All of these metrics will help us locate targets in our radar network along with additional information, such as their size and shape.

1.4 Methodology

We have organized our report in the following way:

Table 1: Outline of the design report

Sections	Topics Covered
	**Section 1** includes problem statement, motivations for the research work done, goals of our design project, and the methodology i.e. the organization of the report.
	**Section 2** covers the background information of this research: literature review, which includes the previous work done in the field of radar imaging. It also includes ethical considerations, codes and standards, economics, safety, etc.
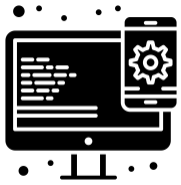	**Section 3** talks about various design requirements like performance, usability, functional decomposition, etc. Section 2 and 3 are somewhat merged because this project has been done completely on software, and we did not have as many design requirements such as costs or materials needed for our project.
	**Section 4** discusses different chaotic systems and their drawbacks and how we choose one over the other because it offers many more advantages, such as higher frequency oscillations, enhanced target detection capabilities, and generating high-resolution radar imaging.
	**Section 5** consists of our preliminary proposed design of Lang-Kobayashi chaotic system, but we also discuss our testing results and include discussion related to why we chose a particular method to generate laser chaos over other methods. We discuss different metrics used to compare three semiconductor laser systems, and their pros and cons. This helped us reach our final design and implementation stage.

	**Section 6** discusses our final design implementation. It includes all the figures, equations, and any other information that might be necessary for the reader to understand the project coherently. We describe the modeling of our system in MATLAB using different functions and mathematical expressions. We also ran simulations for our correlation analysis to establish that our project goals were met by our final design implementation.
	**Section 7** describes the results and discussion based on our final design implementation, what equations did we use, what plots did we generate, what metrics did we study and compare to obtain radar network synchronization, how did it help detect targets, how good was our computation for detecting multiple targets in close proximity, etc.
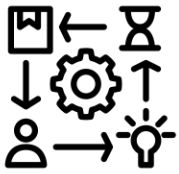	**Section 8** lays out our production schedule, and shows how we stuck to it for most of the part. Sometimes coding different sections took time, so we got behind schedule, but we still managed to accomplish all the tasks given the timeframe.
	**Section 9** discusses the market costs of different hardware components if someone wanted to prototype our system using those equipment. Our project is all documented on software using MATLAB. Hence, we did not incur any costs. But it is important to see how it can be implemented in real-world and what the costs would look like.
	**Section 10** depicts the user's manual and how they can test the system out using MATLAB or in reality, how they can see the application of the network designed.
	**Section 11** consists of the discussion of main points pertaining to the project, conclusion of our report, and the future steps we might take to implement the rest of the project. We will also offer some recommendations to improve the performance of our system.
	**Section 12** consists of all the references and citations related to our research.

2. Background

2.1 Literature Review

This research analyzes the use of multi-static radar instead of monostatic or bistatic radar. A monostatic radar configuration has the receiver and transmitter at the same location(Fig.1). This configuration makes the radar vulnerable to intentional interference and electronic countermeasures (ECMs) [1]-[2].

Instead, a bistatic radar configuration has the transmitter and receiver separated from each other(Fig.2). Thus, the receiver nodes are passive and undetectable. This helps reduce radar's vulnerability to ECMs while detecting targets with low radar cross-sections (RCS) [1]-[3]. However, the bistatic radar configuration is sensitive to its geometry making it tricky to detect targets [25].

Hence, we move towards a multi-static radar network. This configuration consists of multiple transmitters and multiple receivers (Fig.3), which help view targets from different angles. It consists of a single chaotic (driver) oscillator that helps generate multiple chaotic waveforms by changing its initial condition (seed). In addition each site consists of an identical chaotic oscillator. The generated waveform can be used at an individual transmitter (Fig.3). The multistatic radar network offers many advantages over the traditional monostatic radar, such as improved target detection and extraction of target-related information due to differences in the properties of clutter and a higher degree of freedom[1]-[3].

To fully utilize its advantages, a multistatic radar network needs to transmit and receive orthogonal waveforms[5]. Though these waveforms can yield better performance,

they have practical limitations in terms of generation. We can overcome this constraint by using chaotic waveforms that can not only be generated easily[6] but also possess self-synchronization capabilities. These waveforms are pseudo-random with bounded amplitudes. Hence, chaotic samples are highly uncorrelated making them robust in the presence of noise and interference. Besides, they possess a low probability of intercept properties due to their wideband nature[6].

Chaotic systems generate nonlinear waveforms that are aperiodic, bounded, deterministic, and very sensitive to initial conditions. Due to these properties, chaotic systems have been used for secret communications and radar imaging. This is demonstrated in [5] and [6]. Typically, chaotic signals were generated using discrete iterated-maps [5] or continuous nonlinear differential equations [5]. However, in this research, we will generate wideband chaotic signals using the delay differential equations. We will talk about this later in the report.

2.2 Previous work done

Previously, Fan-Yi Lin et al [4] worked on laser chaotic systems for radio detection and ranging (RADAR) correlation analysis. They showed that the correlations obtained using these signals are very sharp with minimum side-lobe levels. Berenice et al., [8] used a similar system called Lang-Kobayashi for laser detection and ranging (LADAR) systems. In this work, targets such as airplanes were detected and classified along with high-resolution images. Willsey et al[6] used chaotic AM signals for radar applications. They were able to produce the waveforms with low autocorrelation sidelobes and limited spectral leakage. This further motivated Flores et al[2-4] to use chaos to generate FM

signals that have large bandwidth that is required for high-resolution radar imaging. Additionally, Carroll [19] used chaotic signals to synchronize a bistatic radar system and optimize it for complex target detection. In this report, we will show how we synchronized a multistatic network and used that for target detection.

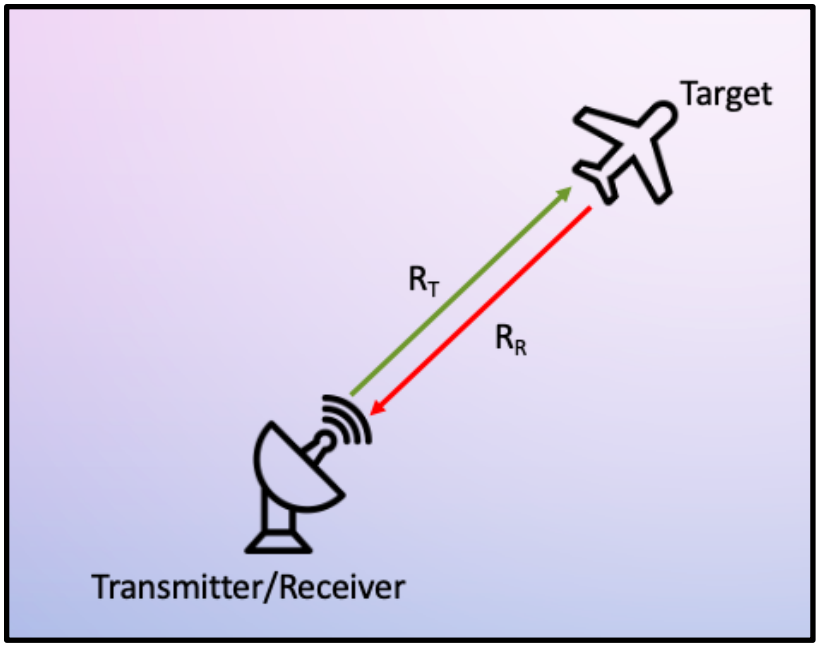

Figure 1: Monostatic Radar Configuration

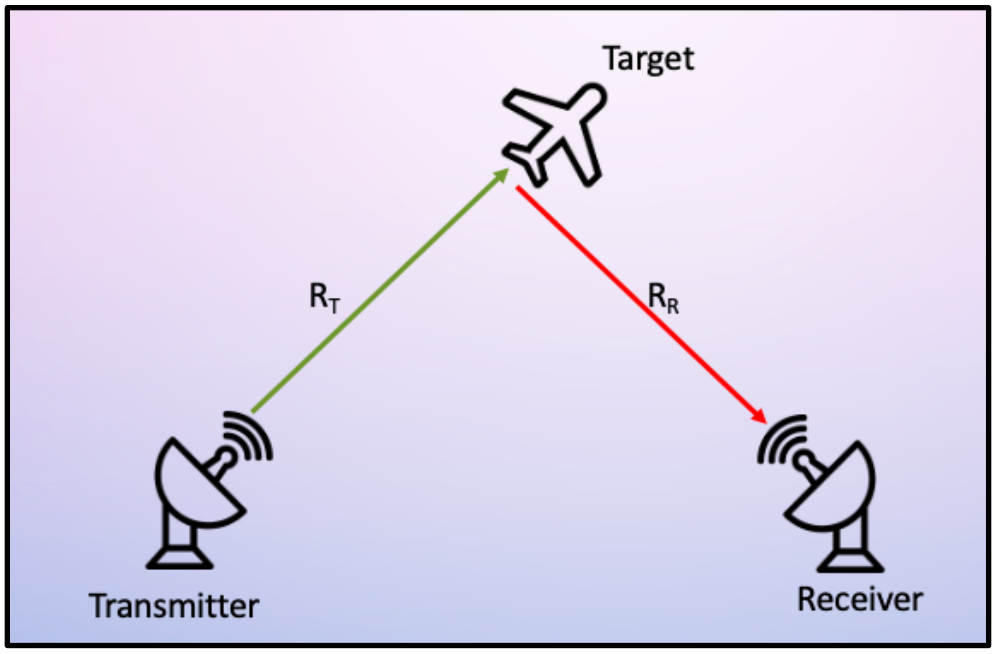

Figure 2: Bistatic Radar Configuration

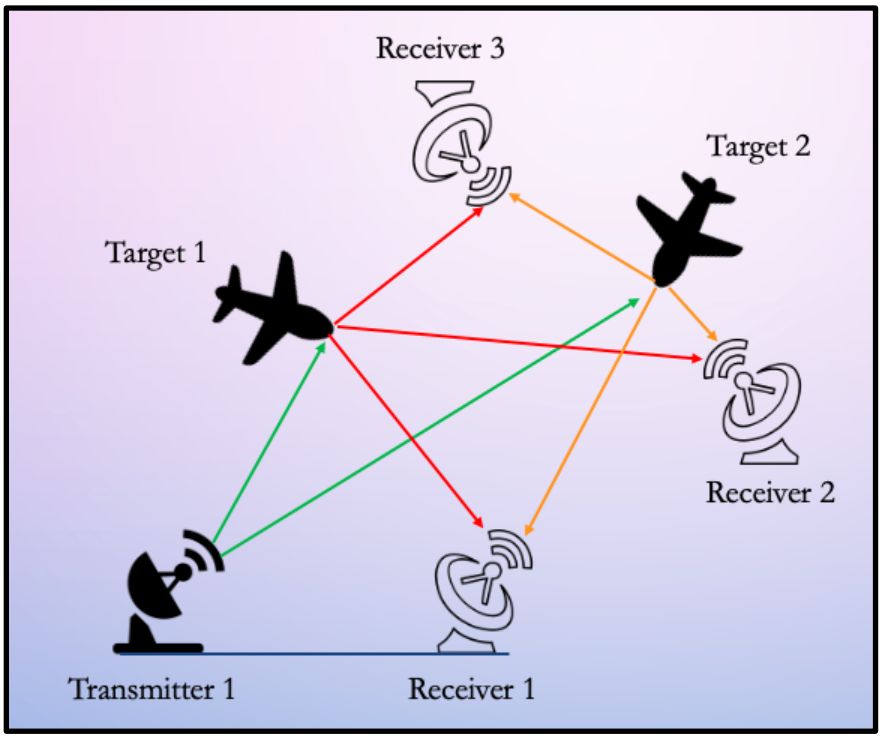

Figure 3: Multistatic Radar Configuration

2.3 Ethical Considerations

In order to successfully implement this project, there are some ethical considerations I need to keep in mind. Once developed, we need to make sure that our constructed radar does not cross-interfere with other wireless devices. We also need to follow the rules set by the Federal Communications Commission (FCC). Details of these rules can be found here [26].

Firstly, since my project is intensively research-based, it is important to specify the research question and correlate the results of the project with the subject that is being explored. This validates our research-oriented project and informs the public about what we are investigating and obtaining.

Secondly, since we are collaborating with Dr. Fan-Yi-Lin[4] from National Chiao Tung University, Taiwan, we need to ensure that we honestly and accurately mention and credit his work on the research. The same goes for previous IEEE researchers who might have done some research in the same area. Although this research is unique in its own way, the sources used to design and implement it must be cited.

Thirdly, since we are working with multi-static radar networks, we need to ensure that we do not cross the frequency range they shall operate in. If we go above the range of 10 - 15 GHz with huge power densities of the radio frequencies emitted by radar systems, it could affect human beings and lead to health hazards[12]. Since our project is being modeled and implemented on software, our major issue would be the interference caused by the high-frequency ranges. Rather than being a health hazard, it would be an ethical consideration in our case.

Lastly, since we are studying radar network synchronization and imaging using semiconductor laser chaos, we need to make sure that we are abiding by the IEEE standards [12-

14] specified for software simulations, radar transmission, and various frequency bands a multi-static radar can operate in (Section 3). Therefore, we are establishing the safety of people and keeping in mind the ethical considerations we need to comply with for our project.

3. Design Requirements

3.1 Detailed Design Specifications

In this section, I will be discussing various aspects of the project, such as its performance, usability, economic feasibility, codes and standards, ethical and legal considerations, and any safety measures one might need to take while implementing it. I am currently doing this project on MATLAB but will be discussing requirements particular to real-world implications.

Usability: This project is completely based on software; however, we can implement this on automated vehicles and see the potentials of laser chaos. We can also use different types of semiconductor lasers or build prototypes to contrast the results of hardware vs. software systems. These semiconductor laser systems can also be used to synchronize multiple transmitters and receivers in our radar network, which can help detect radar targets in our surroundings.

Performance: This project's design is based on that of a chaotic oscillator. Earlier ordinary differential equations were used to generate chaos, we use delayed differential equations for semiconductor chaotic systems with varying control parameters. These control parameters will help to achieve optimized chaotic waveforms. We also plan to use waveforms that possess pseudo-random nature so that we obtain a wideband spectrum with a frequency span of a few GHz. By synchronizing our radar network, we expect it to generate high-quality signals that can be used for detecting low radar cross-sectional targets while preventing any interference in our system[1-3].

Economics: This project will be done completely on MATLAB to obtain radar imaging and synchronize our radar network. Hence, it is free of cost and can be used by people who have access to MATLAB. However, when implemented in the real world, people would have to spend on

hardware components if they wish to test the system out after prototyping a semiconductor laser system. They could also invest in any automated vehicles to see if it can detect and generate high-resolution imagery of a radar target using the concept of laser chaos.

Safety: This project does not have any power source except a desktop or laptop with MATLAB software installed. The human contact would be to run the program to obtain the results. A typical laser system might interfere with a radar system, but that is why we are using chaos in this project. Still, while experimenting and running different tests on various chaotic systems, we want to make sure we abide by specific frequency bands to avoid cross-interference. This is why we have also defined the IEEE standards below, which we will abide by while working on this project.

IEEE Standards: There are various IEEE standards that our project has to comply with to ensure its functionality, validity, design, and implementation. Our project abides by the following standards:

1) **IEEE Std 521 - 2019 (Revision of IEEE Std 521 - 2002) - IEEE Standard Letter Designation of Radar-Frequency Bands**

This standard provides the radar-frequency band letter designations to describe the band in which the radar operates (Table 2). The letter designations help distinguish between a wide variety of radar systems because each frequency band depicts a particular nature of that radar system[12]. Each radar has different characteristics, applications, and environmental constraints illustrated by its frequency bands. This standard helps in maintaining the safety of our environment because it is inadvisable to go above a specified frequency range for the radar system we develop and use. The purpose of this standard is to ensure that engineers do not cross a specific radar-frequency band limit and consequently risk our environment [12].

Table 2: Radar Frequency Bands according to IEEE standards

Band designation	Frequency range	Explanation of meaning of letters
HF	0.003 to 0.03 GHz	High Frequency[11]
VHF	0.03 to 0.3 GHz	Very High Frequency[11]
UHF	0.3 to 1 GHz	Ultra High Frequency[11]
L	1 to 2 GHz	Long wave
S	2 to 4 GHz	Short wave
C	4 to 8 GHz	Compromise between S and X
X	8 to 12 GHz	Used in WW II for fire control, X for cross (as in crosshair). Exotic.[12]
K_u	12 to 18 GHz	Kurz-under
K	18 to 27 GHz	Kurz (German for "short")
K_a	27 to 40 GHz	Kurz-above
V	40 to 75 GHz	
W	75 to 110 GHz	W follows V in the alphabet[citation needed]
mm or G	110 to 300 GHz[note 1]	Millimeter[10]

Since our project deals with radar systems and radar transmission, it is important to ensure that we do not cross the frequency band limit specified for it.

2) **IEEE Std 686 - 2017 (Revision of IEEE Std 686 - 1997) - IEEE Standard for Radar Definitions**

This standard provides radar definitions as radar technology and literature keep evolving. The purpose of this standard is to promote clarity and consistency in the use of radar terminology. The purpose of the revision of the previous standard is to add new terms, delete obsolete terms, and revise others to maintain the present radar system terminology [13].

This is extremely significant for our project because it should abide by the current radar uses and technology to design and implement the synchronization and imaging of our radar network.

3) **IEEE Std 829 - 2008 - IEEE Standard for Software and System Documentation**

This standard establishes a common framework for testing processes, activities, and tasks in support of all software life cycle processes including acquisition, supply, development, operation, and maintenance. The purpose of this standard is to ensure that when we are testing our system using computer software, we shall document our testing plan, design specifications, the input and output of the system, the breakdown of tasks the system has to accomplish, and the outcome of the system we are modeling and testing using the computer software [14]. In our case, we are using MATLAB for all the testing, modeling, and generating purposes.

3.2 Functional Decomposition of the project

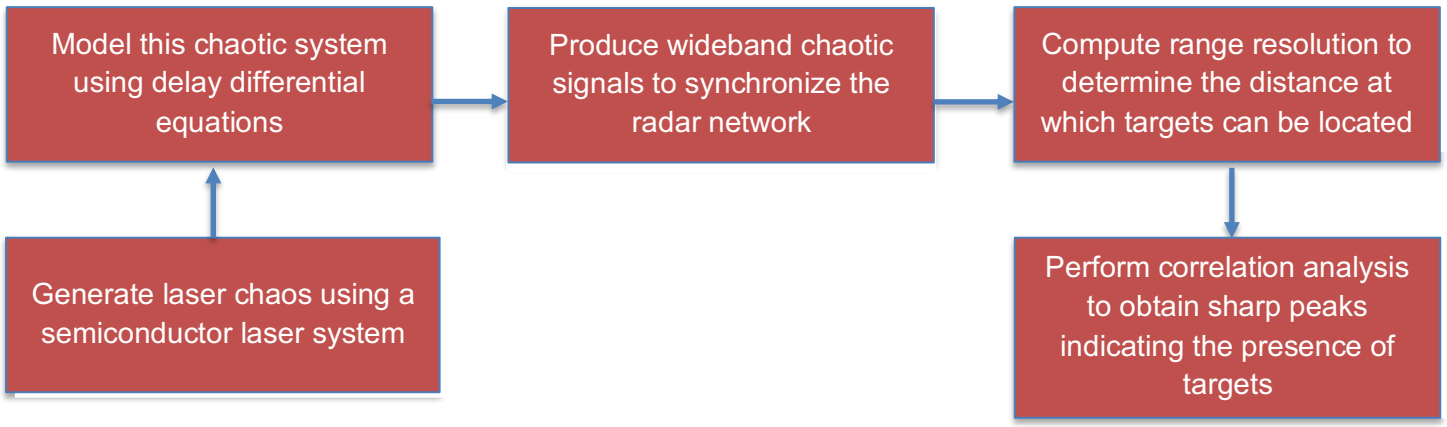

Figure 4: Function Decomposition of our system

The current radar systems use additional hardware stated in Section 1. We are replacing those equipment with a semiconductor laser system, which helps reduce noise within the system while generating wideband chaotic signals. This also reduces the clutter and cost of the system[1-3].

The system generated using semiconductor laser chaos, as we will see later in the report, is able to generate waveforms in the range of 0-10 GHz while not crossing the frequency band limit set by the IEEE standard i.e. 10-15 GHz [12]. The transmitter and receiver need to be

synchronized so that the system can detect multiple targets efficiently. The overall noise factor between the transmitter and receiver should be less than -13.3 dB to prevent any kind of interference and avoid false alarms. As stated in section 2.3 and 3.1, we need to remain within the legal range of frequencies to avoid any health hazards that can be caused due to very high frequencies. This helps ensure safety of people and our surroundings. The IEEE standards set the rules and regulations for the system and how we need to document our simulations, testing procedures, and design requirements. This would help a potential user understand how the system works and how they can test the system to validate our findings.

4. Design Alternatives

When we came up with the idea of using laser chaos to detect targets, we had to investigate and simulate various chaotic systems and observe which system fulfilled our requirements. In this section, we will report our findings based on different chaotic systems, their drawbacks, and how we chose the final system to generate laser chaos to successfully synchronize a multistatic radar network.

4.1 One-Dimensional Chaotic Maps

The first type of chaotic systems we studied are the one-dimensional chaotic maps. We analyzed the Logistic and the Bernoulli maps, and we will present our results for both in this section.

Logistic map is defined using the following equation: $x_{n+1} = rx_n(1 - x_n)$

We modeled the above equation in MATLAB using r=0.4, and obtained the following plot of the attractor of the Logistic map:

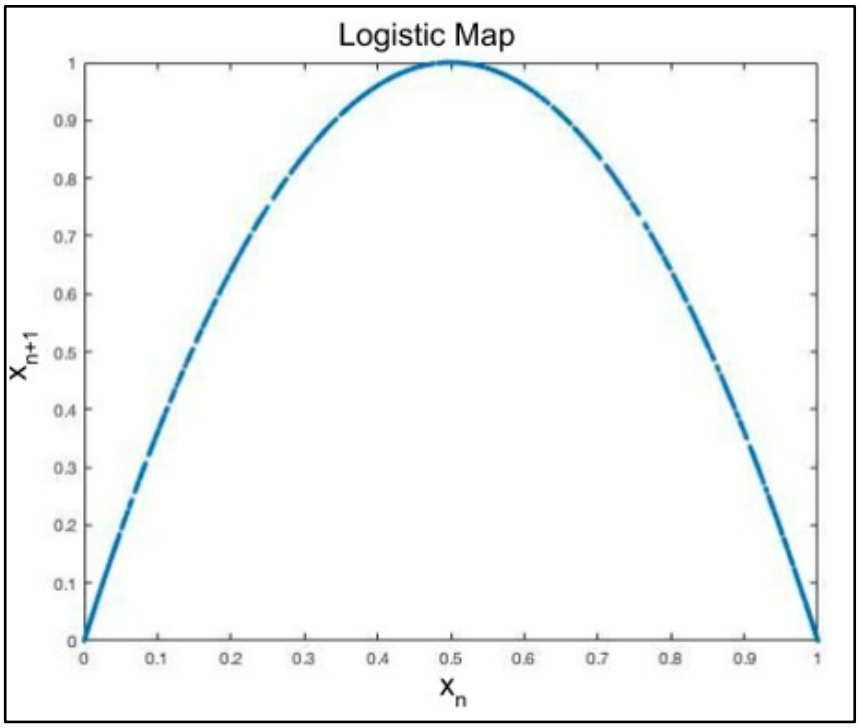

Figure 5: Attractor of the Logistic Map

Logistic map uses the aforementioned nonlinear difference equation to look at discrete-time steps[16].

Another type of chaotic map is the Bernoulli map, which is modeled using the following equation: $x(n+1) = Bx(n) + A\ if\ x(n) < 0;\ x(n+1) = Bx(n) - A\ if\ x(n) > 0$

Here, A=0.5 and B=1.999. We modeled these equations in MATLAB and obtained the following plot:

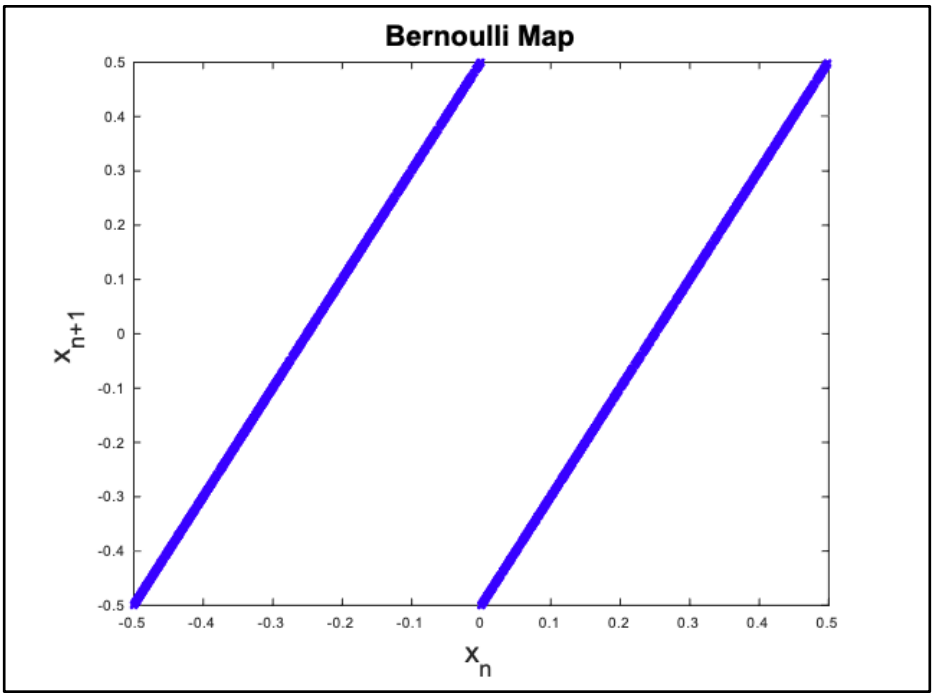

Figure 6: Bernoulli Map

Both of these maps depict chaotic behavior but have various drawbacks. They often pose complications in signal transmission due to their discrete-time nature and usage of single waveforms instead of multiple waveforms (Fig.5 and 6). Due to their lack of efficiency in signal transmission, they cannot be used to detect targets or obtain their imagery. Thus, we explore another chaotic system - the Lorenz system.

4.2 Lorenz System

The Lorenz system is a continuous chaotic system. It can be defined mathematically by a set of nonlinear differential equations that were first studied by Edward Lorenz[16]. These equations are as follows:

$$\frac{dx}{dt} = \sigma(y - x)$$

$$\frac{dy}{dt} = x(\rho - z) - y$$

$$\frac{dz}{dt} = xy - \beta z$$

These equations were developed by Lorenz to model atmospheric convection. Here, 'x', 'y', and 'z' are the chaotic state variables and σ=10, β=8/3, and ρ=28 represent the control parameters that govern the dynamical system [15]. These control parameters determine the chaotic nature of the system. We modeled the aforementioned equations in MATLAB using ODE45 function, and obtained the following plot:

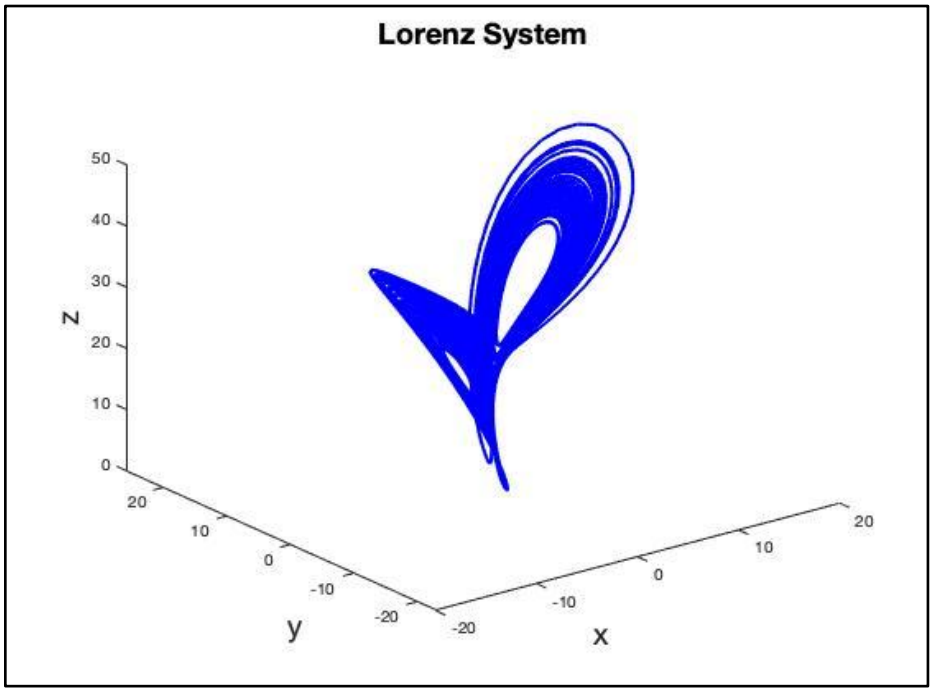

Figure 7: Lorenz System

4.2.1 Interpretation of the Lorenz System

As we can see from Fig.7, the Lorenz System has two wings. These wings represent two different sets of the physical behavior of the system [16]. A point on that graph represents a

particular physical state, and the blue curve is the path followed by such a point during a finite period. If we observe Fig.7 closely, we also see that the system keeps spiraling from one wing to the other. The line making up the curve never intersects itself and never retraces its path [16]. Instead, it loops around forever and this is what depicts the randomness and unpredictability of the system. Both of these properties make the Lorenz System chaotic too.

4.2.2 Sensitivity to initial conditions and its significance in the field of radar

The Lorenz System depicts other chaotic properties such as being aperiodic, bounded, deterministic, and sensitive to initial conditions[16]. We can observe that from the following figures:

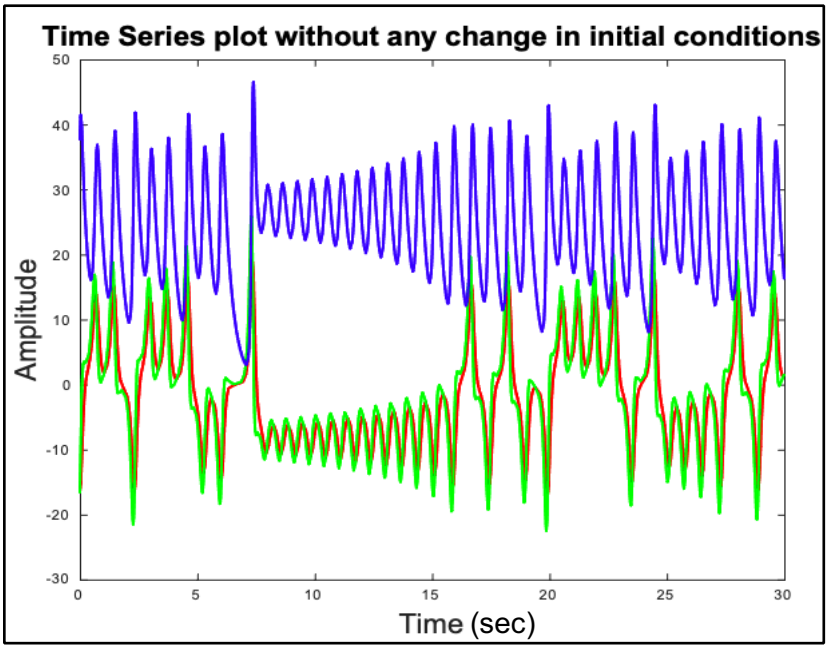

Figure 8: Time series plot of Lorenz system without any change in initial conditions

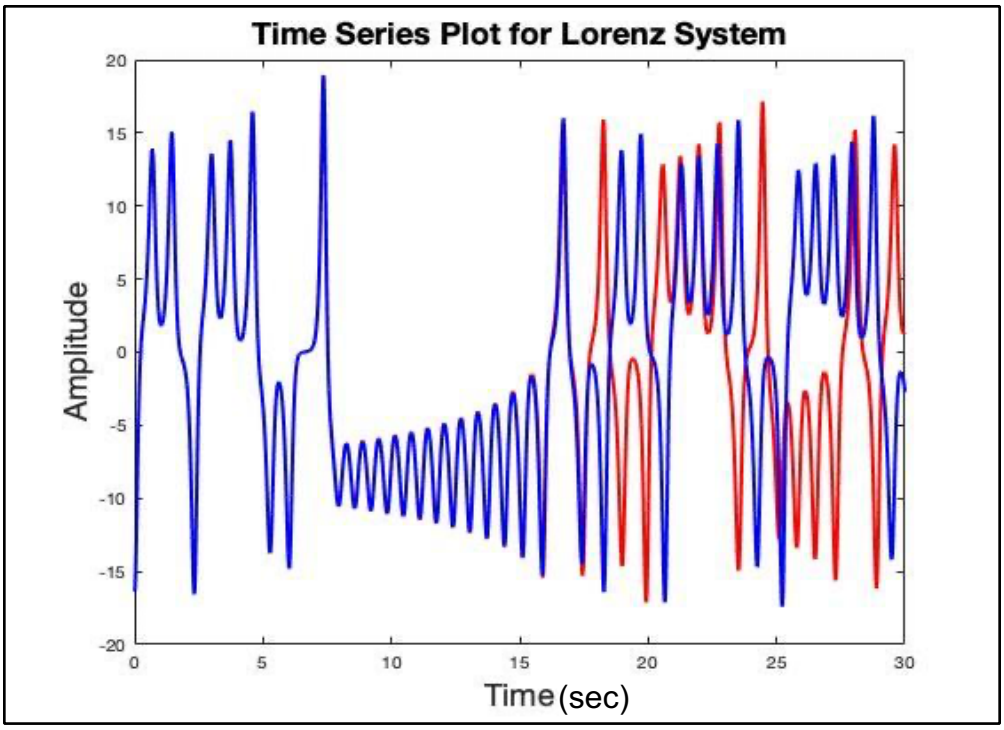

Figure 9: Sensitivity to initial conditions in case of Lorenz attractor

The blue time series plot represents the output of the Lorenz attractor when x = -16.3715, y = -16.6979, z = 37.6179; the red spectrum, which diverges, is the output of the Lorenz attractor when we add a factor of 10^{-9} to x, y, and z. From Fig. 9, we can see how a small change in initial conditions leads to a huge divergence of the waveform.

This property of chaotic systems is what makes them possess pseudo-random properties. This is also what makes them much more beneficial as compared to Linear FM signals (LFM) which can be easily detected by intruders and electronic intelligent systems(ELINTS) that can create false alarms at the radar receiver[1-3]. However, chaotic signals help prevent these problems and can never be repeated because of their sensitivity to initial conditions. This makes them undetectable by ELINTS or other intruders[1-3].

4.2.3 Drawbacks of the Lorenz System

Even though this system depicts chaotic behavior, it oscillates at lower frequencies because it can't be transmitted directly and it has a non-constant envelope. In order to yield constant-envelope output waveforms that can oscillate at higher frequencies, we will have to modulate the Lorenz system onto frequency. This will help generate chaos-based frequency modulation(CBFM) which will consequently produce wideband chaotic signals. Nevertheless, CBFM requires additional hardware such as voltage control oscillators, amplifiers, and mixers to generate wideband chaotic signals. Thus, we use semiconductor laser systems that can replace the additional hardware while producing signals that oscillate at higher frequencies.

Due to the drawbacks of both one-dimensional chaotic maps and Lorenz system in terms of detecting and generating high-resolution imagery of targets, we study the Lang-Kobayashi system generated using a semiconductor laser system.

5. Preliminary Proposed Design

5.1 Lang-Kobayashi System

The Lang-Kobayashi system is defined by the following delayed-differential equations[4]:

$$\frac{da_T}{dt} = \frac{1}{2}\left[\frac{\gamma_c\gamma_n}{\gamma_s J} n_T - \gamma_p(2a_T + {a_T}^2)\right](1 + a_T) + \xi_i\gamma_c cos(\Omega t + \phi_T) \quad (1)$$

$$\frac{d\phi_T}{dt} = \frac{-b}{2}\left[\frac{\gamma_c\gamma_n}{\gamma_s J} n_T - \gamma_p(2a_T + {a_T}^2)\right](1 + a_T) - \frac{\xi_i\gamma_c}{1+a_T} sin(\Omega t + \phi_T) \quad (2)$$

$$\frac{dn_T}{dt} = -\gamma_s n_T - \gamma_n(1 + a_T)^2 n_T - \gamma_s J(2a_T + {a_T}^2) + \frac{\gamma_s\gamma_p}{\gamma_c} J(2a_T + {a_T}^2)(1 + a_T)^2 + \xi_f\gamma_s(J + 1)(1 + a_T(t - \tau))^2 \quad (3)$$

In the aforementioned deterministic rate equations, "a" is the normalized field, "ø" is the optical phase difference, and "ñ" is the normalized carrier density[4]. We refer to these equations as delay differential equations because the term $a(t - \tau)$is a delay term. These equations are modeled using MATLAB's DDE23 function. The figure below shows the phase space plot obtained between 'a' and 'n':

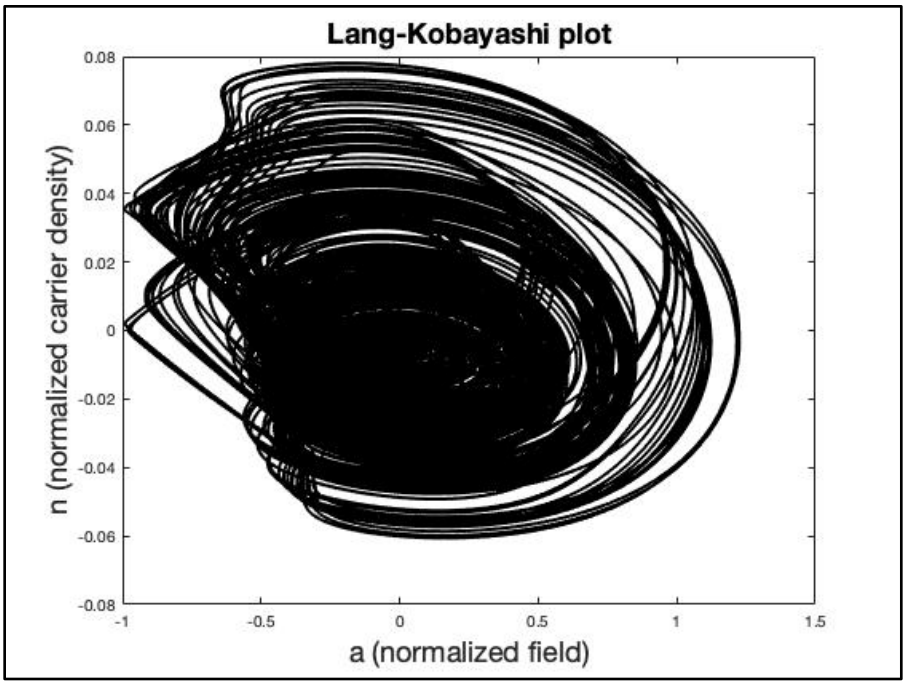

Figure 10: Phase space plot of the Lang-Kobayashi system

5.2 Properties of the Lang-Kobayashi plot

As we can see from Fig.10, the phase space plot of the Lang-Kobayashi system generated using a semiconductor laser system has an attractor behavior. The advantage of this system is that it oscillates at higher frequencies, consequently generating wideband chaotic signals.

5.3 Sensitive Dependence of transmitted signal

The transmitted waveform generated by the Lang-Kobayashi system is modeled as $s = (1 + a)^2$. In Fig.11, we can see that the blue time-series plot is diverging from the red time-series plot when we change the initial conditions by a very small factor of 10^{-9}. This shows the transmitted signal's sensitivity to initial conditions, depicting the chaotic behavior of the Lang-Kobayashi system.

In the next section, we will discuss two metrics - Power Spectral Density and Autocorrelation - to analyze the Lang-Kobayashi system's wideband spectrum and range resolution capabilities. This will help validate our choice of using this system for target detection and imaging purposes.

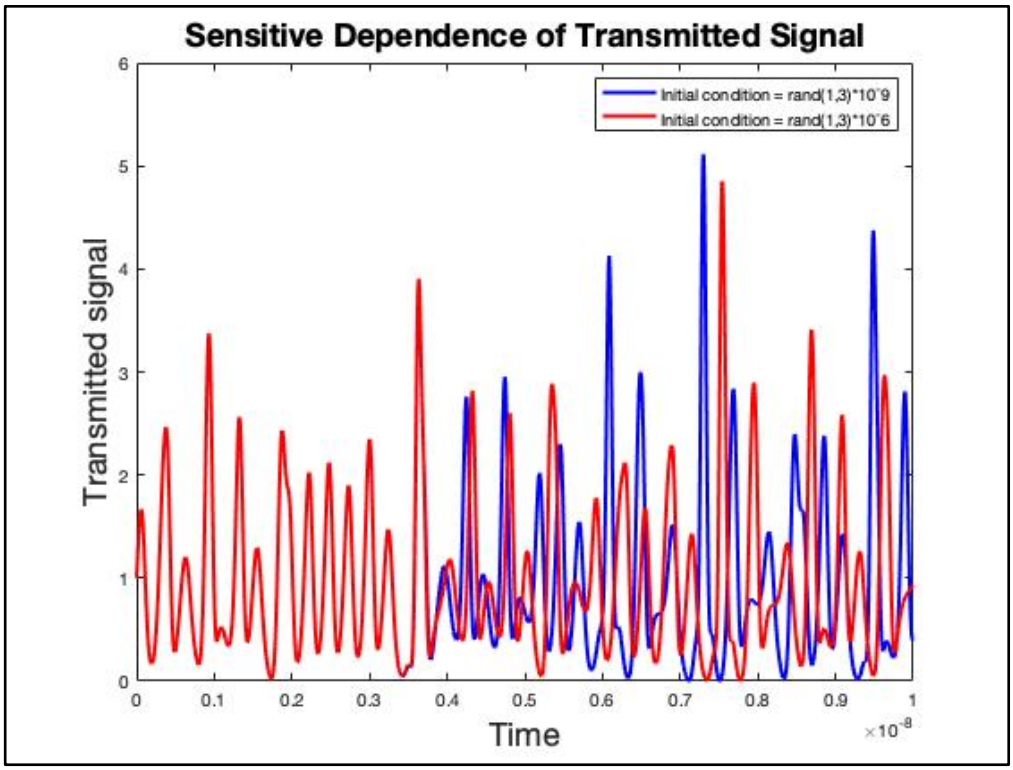

Figure 11: Sensitive Dependence of Transmitted signal of Lang-Kobayashi system

5.4 Power Spectral Density

Power Spectral Density is used to measure the signal's power content in terms of the frequency [29]. We also define it as the Fourier transform of the autocorrelation of the transmitted signal [29]. It is mathematically expressed in the following way:

$$\lim_{T\to\infty} \int_{-\infty}^{+\infty} \frac{|S_T(f)|^2}{T} df$$

In the above equation, S(f) is the transmitted signal [29].

In order to obtain the high-resolution imagery of a radar target, it is important to study the correlation performance. Power Spectral Density is used to assess the spectral spread of a given waveform. We will present our testing results using all three types of semiconductor lasers to see which system gives the best correlation performance.

5.5 Autocorrelation of the transmitted signal

Autocorrelation is defined as the convolution of a signal with a time-reversed version of itself [28]. Mathematically, we describe it as follows:

$R(\tau) = \lim_{T\to\infty} \int_{-T/2}^{T/2} g(t)g(t-\tau)dt$ where g(t) is the transmitted signal [29].

A sharp correlation peak helps determine the quality and capability of a signal in achieving high-resolution imagery of the targets. The peak of the autocorrelation plot indicates the location of the target. In order to differentiate between different laser systems, we will see if we get a sharp autocorrelation peak with minimum sidelobes.

5.6 Testing of our preliminary proposed design

In this section, we will subject our Lang-Kobayashi system to three different types of semiconductor laser systems: Optical Feedback (OF), Optoelectronic Feedback (OEF), and Optical Injection (OI) methods. We will be studying the effect of each laser system on our transmitted signal using different metrics (mentioned in Section 4.4 and 4.5). In section 5.6.1, we will show how each method is modeled and what our results for power spectral density and autocorrelation look like. In section 5.6.2 and 5.6.3, we will discuss the results obtained from our simulations to choose the most efficient semiconductor laser system.

5.6.1 Introduction of different types of semiconductor lasers:

1. **Optical Feedback**:

This method has been used to generate chaos for various applications like secure communications, random bit generation, radar, lidar, and image encryption[18]. It offers the advantages of simple configuration and lower costs in contrast to optoelectronic feedback and optical injection[18].

It is modeled using the following equations [18]:

$$\frac{da}{dt} = \frac{1}{2}\left[\frac{\gamma_c \gamma_n}{\gamma_s J} n - \gamma_p(2a + a^2)\right](1 + a) + \xi\gamma_c[1 + a(t - \tau)]cos[\phi(t - \tau) - \phi(t)]$$

$$\frac{d\phi}{dt} = -\frac{b}{2}\left[\frac{\gamma_c \gamma_n}{\gamma_s J} n - \gamma_p(2a + a^2)\right](1 + a) + \xi\gamma_c\left[\frac{1 + a(t - \tau)}{1 + a}\right] sin[\phi(t - \tau) - \phi(t)]$$

$$\frac{dn}{dt} = -\gamma_s n - \gamma_n(1 + a)^2 n - \gamma_s J(2a + a^2) + \frac{\gamma_s \gamma_p}{\gamma_c} J(2a + a^2)(1 + a)^2$$

Here, 'a' is the normalized optical field, 'ϕ' is the optical phase, 'n' is the normalized carrier density, 'ξ' is the normalized feedback strength, and 'τ' is the feedback delay time[18]. I have included a table below to show each parameter's value and how we modeled our system using this method.

Table 3: Optical Feedback Parameters

Symbol	Meaning	Value
γ_c	Cavity Decay Rate	5.36×10^{11} s^{-1}
γ_s	Spontaneous Carrier Decay Rate	5.96×10^{9} s^{-1}

γ_n	Differential Carrier Relaxation Rate	7.53×10^{9} s^{-1}
γ_p	Non-Linear Carrier Relaxation Rate	1.91×10^{10} s^{-1}
b	Linewidth Enhancement Factor	3.2
$\boldsymbol{\tau}$	Delay Time	1 ns
$\boldsymbol{\varepsilon}_f$	Feedback Parameter	0.09
J	Normalized Bias Current Parameter	1.222
f_r	Resonance Frequency	10.25 GHz
$f = \Omega/2*\pi$	Detuning Frequency	5 GHz

We used the aforementioned equations with their respective values to generate the power spectral density and autocorrelation plots. We obtained the following results:

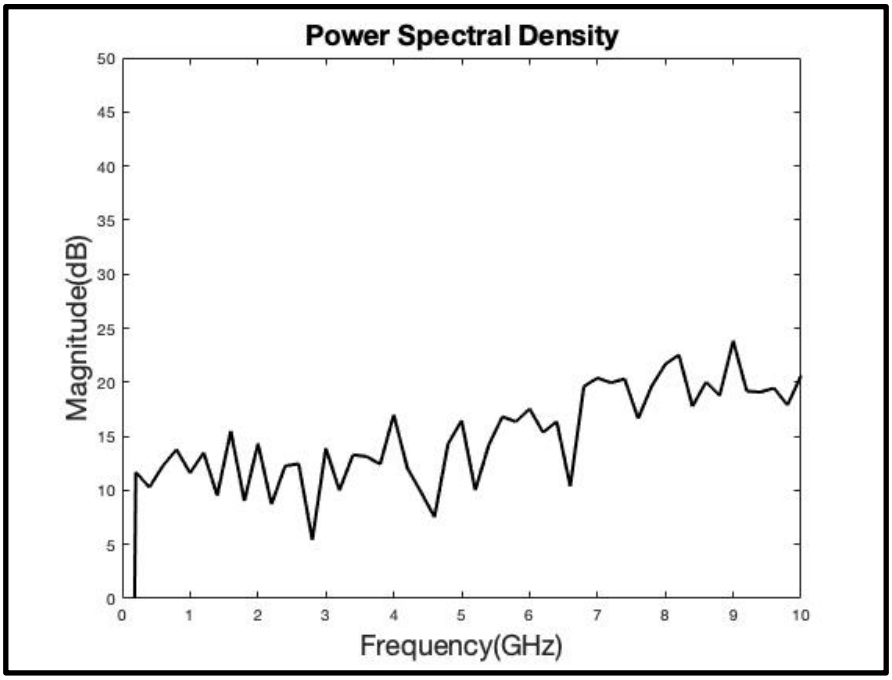

Figure 12: Power Spectral Density for OF

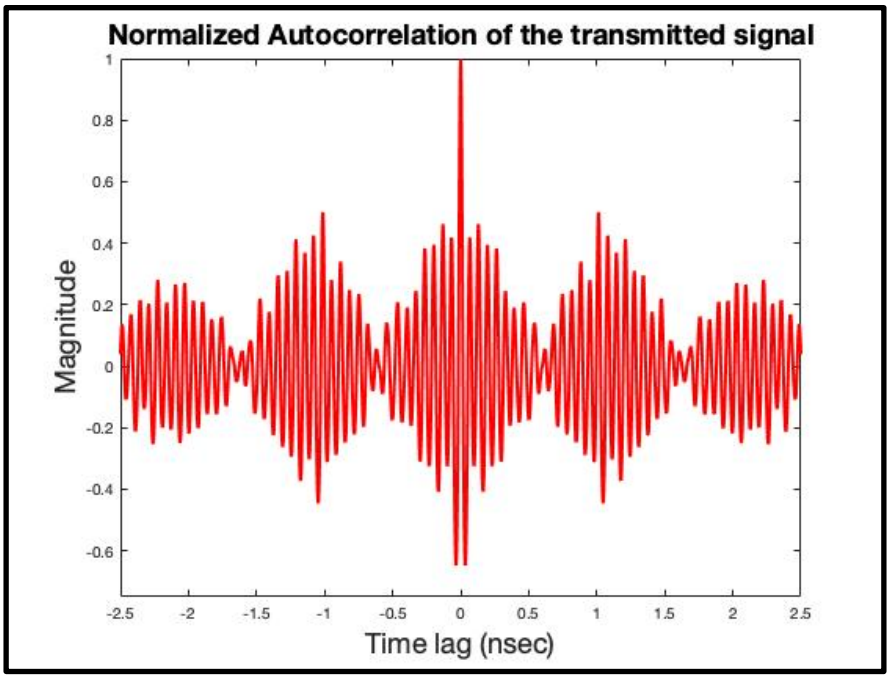

Figure 13: Autocorrelation plot for OF

2. **<u>Optoelectronic Feedback:</u>**

This method is also used to generate wideband chaotic signals that oscillate at high frequencies using the following schematic:

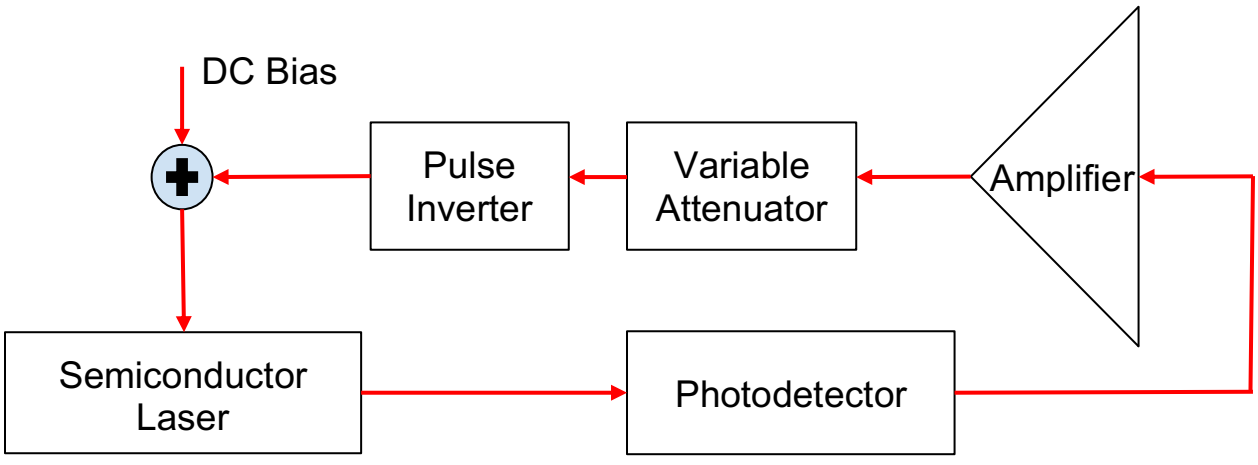

Figure 14: Schematic of Optoelectronic Feedback method

In this method, the output of the semiconductor laser can be either negatively or positively fed back to itself optoelectronically with a time delay [5]. We will present our results using negative feedback (Table 4).

The dynamics of the semiconductor laser are controlled by adjusting the operational parameters, such as the injection current, the feedback strength, and the time delay [5]. In this method, the feedback strength is controlled by the amplifier and the variable attenuator. The delay time, associated with the negative feedback, is adjusted using an optical delay line between the laser and the photodetector[5]. The waveforms are detected and extracted using the photodetector[5]. Lastly, a two-stage amplifier is used to amplify the feedback current detected by the photodetector[5].

We used the following equations to model our optoelectronic feedback method:

$$\frac{da_T}{dt} = \frac{1}{2}\left[\frac{\gamma_c \gamma_n}{\gamma_s J} n_T - \gamma_p (2a_T + {a_T}^2)\right](1 + a_T) + \xi_i \gamma_c cos(\Omega t + \phi_T)$$

$$\frac{d\phi_T}{dt} = \frac{-b}{2}\left[\frac{\gamma_c \gamma_n}{\gamma_s J} n_T - \gamma_p (2a_T + {a_T}^2)\right](1 + a_T) - \frac{\xi_i \gamma_c}{1 + a_T} sin(\Omega t + \phi_T)$$

$$\frac{dn_T}{dt} = -\gamma_s n_T - \gamma_n (1 + a_T)^2 n_T - \gamma_s J(2a_T + {a_T}^2) + \frac{\gamma_s \gamma_p}{\gamma_c} J(2a_T + {a_T}^2)(1 + a_T)^2 + \xi_f \gamma_s (J + 1)(1 + a_T(t - \tau))^2$$

In the above equations, 'a' is the normalized field, 'Φ' is the optical phase difference between the intracavity and injection fields, and 'n' is the normalized carrier density [5]. The table below shows the values for all the parameters and will help us understand how the system is modeled in MATLAB.

Table 4: Optoelectronic Feedback Parameters

Symbol	Meaning	Value
γ_c	Cavity Decay Rate	2.4×10^{11} s^{-1}
γ_s	Spontaneous Carrier Decay Rate	1.458×10^{9} s^{-1}
γ_n	Differential Carrier Relaxation Rate	1×10^{9} s^{-1}
γ_p	Non-Linear Carrier Relaxation Rate	1.2×10^{9} s^{-1}
b	Linewidth Enhancement Factor	4
Ω	Detuning Frequency	$1.445*10^{10}$ Hz
τ	Delay Time	3.24 ns
ε_i	Injection Parameter	0
ε_f	Feedback Parameter	-0.10
J	Normalized Bias Current Parameter	1/3
f_r	Resonance Frequency	2.5 GHz
$f = \Omega/2*\pi$	Detuning Frequency	2.3 GHz
$\tau*f_r$	Normalized Delay Time	8.1 sec

We modeled the equations stated above to generate plots for power spectral density and autocorrelation. We obtained the following results:

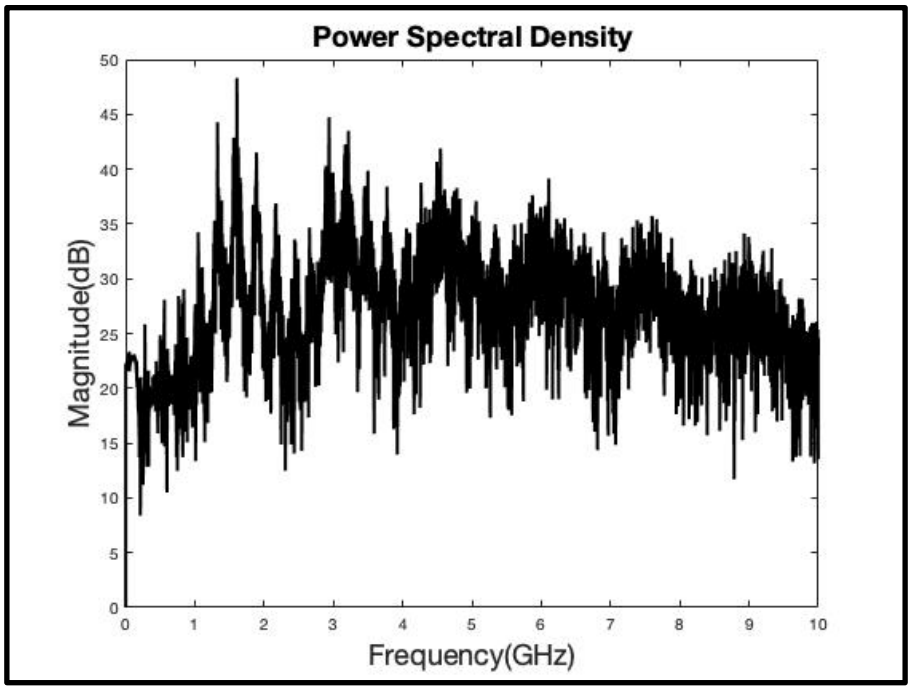

Figure 15: Power Spectral Density for OEF

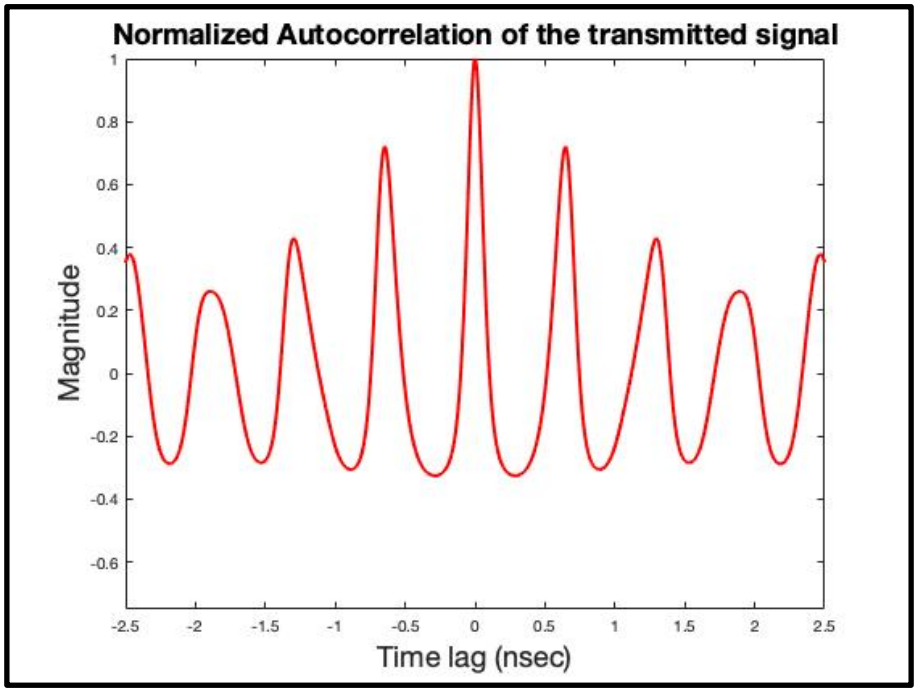

Figure 16: Autocorrelation plot for OEF

3. **Optical Injection:**

This method uses the following schematic to generate laser chaos:

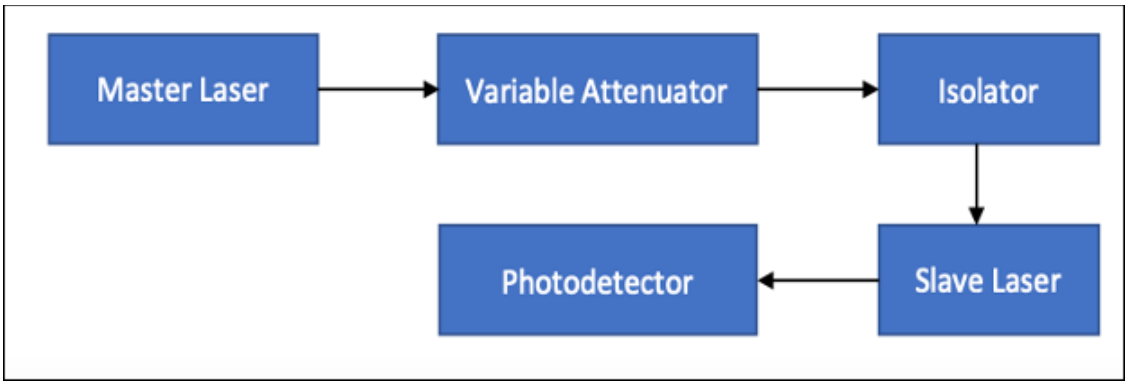

Figure 17: Schematic of Optical Injection method

In this case, the slave laser is optically injected by the master laser. The dynamics of the slave laser can be controlled by adjusting operational parameters, such as the injection current of the slave laser, the detuning frequency between the master and the slave laser, and the optical injection strength from the master to the slave laser[5]. Additionally, the variable attenuator is used to control the injection strength and the isolator is used to prevent any unwanted optical feedback. Lastly, the photodetector is used to detect the output of the slave laser and convert it to an electrical signal [5].

We used the same equations that were used to model the optoelectronic feedback method, but with the following values:

Table 5: Optical Injection Parameters

Symbol	Meaning	Value
γ_c	Cavity Decay Rate	2.4×10^{11} s^{-1}
γ_s	Spontaneous Carrier Decay Rate	1.458×10^{9} s^{-1}
γ_n	Differential Carrier Relaxation Rate	1×10^{9} s^{-1}
γ_p	Non-Linear Carrier Relaxation Rate	1.2×10^{9} s^{-1}
b	Linewidth Enhancement Factor	4
Ω	Detuning Frequency	$1.445*10^{10}$ Hz
τ	Delay Time	3.24 ns
ε_i	Injection Parameter	0.031
ε_f	Feedback Parameter	0
J	Normalized Bias Current Parameter	1/3
f_r	Resonance Frequency	2.5 GHz
$f = \Omega/2*\pi$	Detuning Frequency	2.3 GHz
$\tau*f_r$	Normalized Delay Time	8.1 sec

We modeled the aforementioned equations along with their values in MATLAB to obtain the following power spectral density and autocorrelation plots:

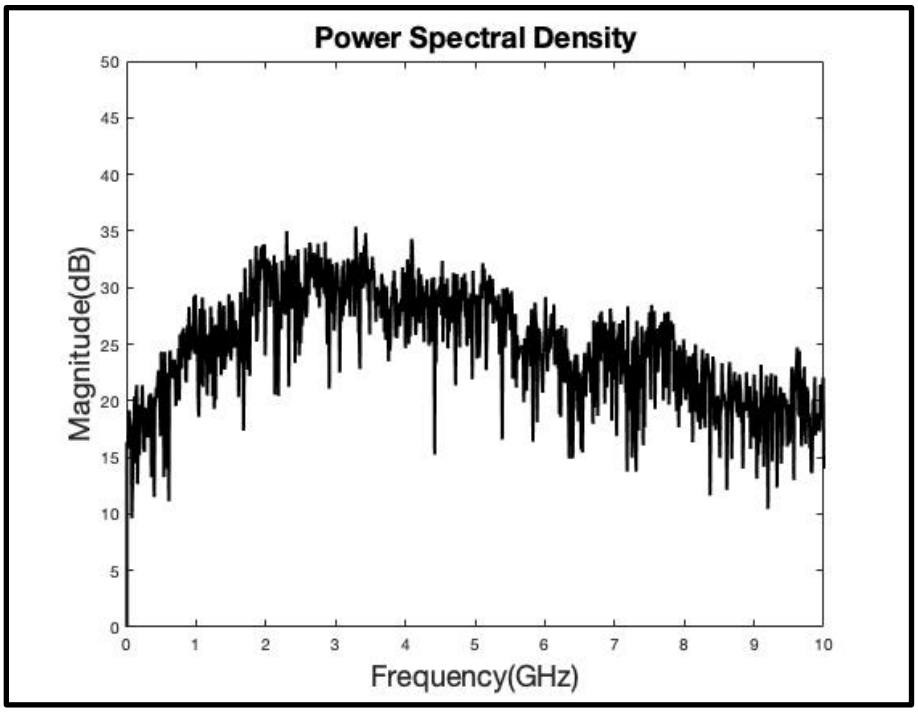

Figure 18: Power Spectral Density for OI

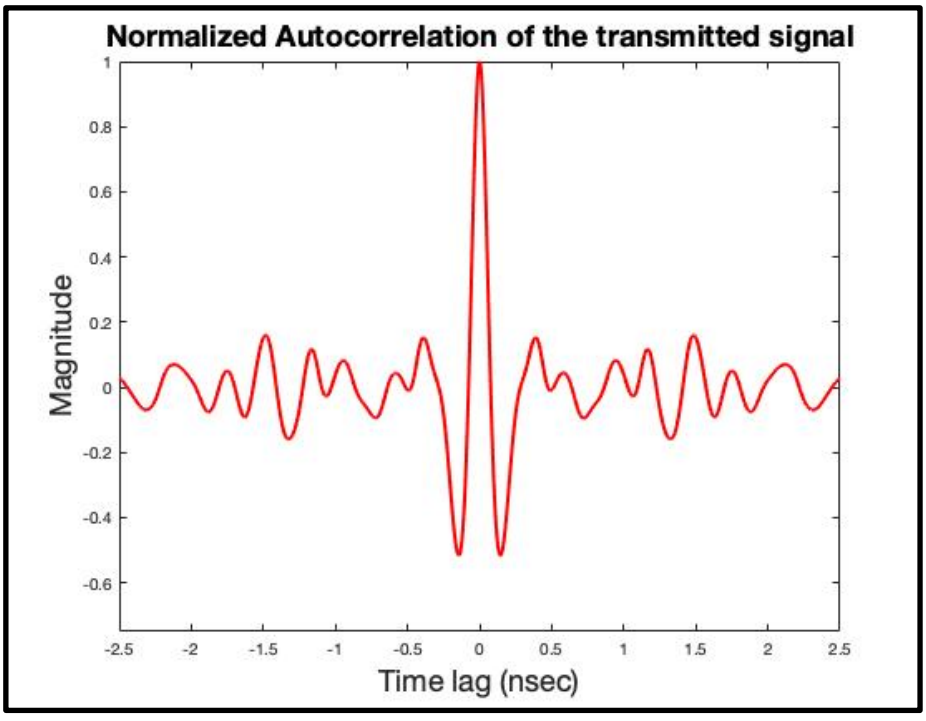

Figure 19: Autocorrelation plot for OF

5.6.2 Discussion of the results for Power Spectral Density

As we can see from Fig.12,15, and 18, all the three laser systems depict a wideband spectrum. All of the generated spectrums span over a range of 0-10 GHz. However, OEF and OI show a flatter spectrum as compared to OF. This doesn't provide us with much information to choose the best system. Thus, we will use another metric - autocorrelation of transmitted signal - to pick the most efficient semiconductor laser chaotic system.

5.6.3 Discussion of the results of autocorrelation

As we can see from Fig.13,16, and 19, the OF and OEF methods have multiple peaks along with high sidelobes. This is not desirable for detecting targets. Additional unwanted peaks indicate the presence of a target when there is no target. This can increase the probability of false alarm at the radar receiver. Also, if we have multiple peaks, we cannot detect the exact location of a target or generate its imagery. Additionally, both these methods show high sidelobes so even if we are able to detect the target, the sidelobes will mask them. Instead, the OI method shows a sharp peak with minimum sidelobes[5]. Thus, we choose the OI method to generate laser chaos, detect targets and synchronize our radar network.

5.7 Range Resolution

As shown in section 5.6, the Optical Injection scheme provides the desirable properties necessary for high resolution radar imaging. The next step is to determine the capability of our waveform to detect closely spaced targets using the OI method. This capability is termed as range resolution, denoted by 'R'[19]. Radar range resolution depends on various factors such as

transmitted pulse width/mainlobe width, beamwidth, type of target, size of target, efficiency of the radar receiver, and resolution of the radar display unit[19]. The equation to calculate range resolution is given below:

$$R = \frac{c\Delta\tau}{2}$$

In the above equation, 'c' is the speed of light = 3×10^8 and τ is the mainlobe width. The mainlobe implies the width of the main peak of the autocorrelation. The width of the mainlobe is computed as the halfpoint(magnitude) width of its peak. It is similar to computing the half power point.

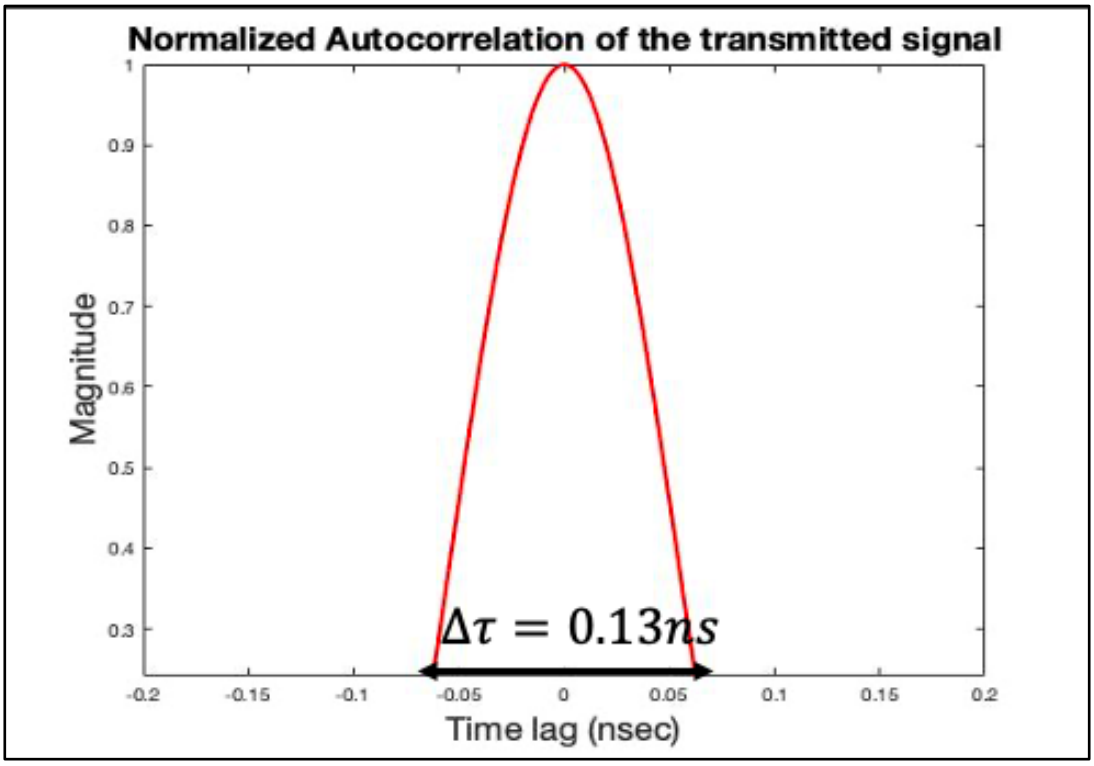

Figure 20: Plot for obtaining the mainlobe width

It is obvious that the mainlobe width is 0.13ns and hence the corresponding range resolution turned out to be 2 cm. This implies that we can detect two closely spaced targets at a distance greater than 2 cm.

5.8 Two-Point target simulation

In order to illustrate the range resolution capabilities of our laser system, we performed a two-point target simulation. This simulation helps us detect multiple targets in close proximity. In our case, we assume that two targets are located at 50 m and 51 m. We performed a cross correlation between our transmitted and received signals, where received signal is $r(t) = \alpha_1 s(t-\tau_1) + \alpha_2 s(t-\tau_2)$. Here, $\alpha_1$and$\alpha_2$are reflection parameters and $\tau_1$and $\tau_2$are delays associated with the signals. We obtained the following plot after doing the cross correlation:

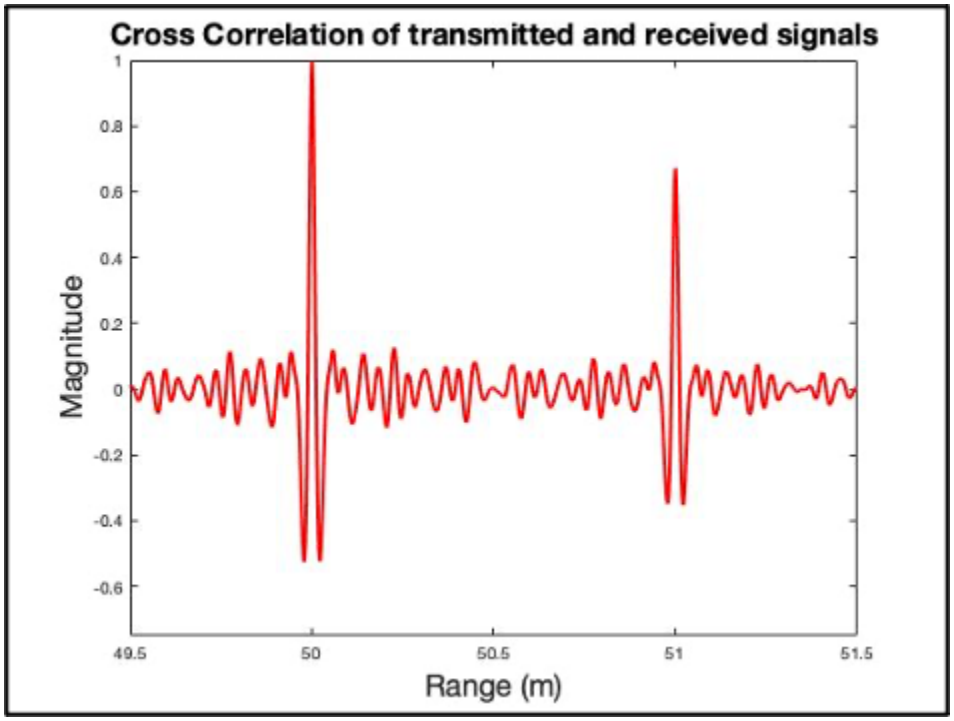

Figure 21: Two-point target simulation

As we can see from Fig.21, our correlation peaks are at 50 and 51m respectively, indicating the location of our targets. Additionally, our targets are separated by a distance of 1m, which is greater than 2 cm. This shows how range resolution and correlation help detect the location of radar targets

efficiently. It also depicts the high quality of our wideband chaotic signals because we obtain sharp correlation peaks.

6. Final Design and Implementation

In this section, we will present our final design of a synchronized radar network and how we implemented it using MATLAB. We will discuss why we synchronize the multistatic radar network and what are some metrics that help us observe a synchronized network.

6.1 Significance of synchronizing a radar network

Synchronization of a radar network helps filter out noise while yielding improved target detection. In the past, several researchers have proposed different methods for synchronizing radar networks. Weib[4] explored the use of navigation systems and two-way communication links to synchronize radar networks. However, all these methods require additional hardware and power requirements. Instead, Carroll[20] proposed the use of analog chaotic circuits to synchronize bistatic radar systems. An advantage of using chaotic oscillators is their ease in building the system and they are less costly compared to alternate synchronization methods (mentioned in Section-). Thus, we use the self-synchronization property of chaos along with the semiconductor laser system to synchronize all nodes in our radar network. The chaotic signals are broad band, so they have good range resolution capabilities[25]. Moreover, the synchronization capabilities of chaos along with the wideband spectral properties help extract additional information about the target, such as its size and shape. In our case, we use a multi-static radar for synchronization because it can prevent intentional interference and obtain location of our targets efficiently.

6.2 Methodology of radar network synchronization

In this section, we will show the process of synchronizing the radar network. Let us consider our Lang-Kobayashi system that exhibits chaotic properties, and has a set of state variables 'a','Φ',

and 'n', and various control parameters shown in Table 3, section 5. From (1),(2), and (3) equations stated in section 4.1, we can use the state variable 'a_T' as the driving function. Let the transmitted waveform from the driver system be $a_T(t)$. Now, $a_T(t)$can be utilized as the driving signal to synchronize the response system, denoted by 'a_R'. Once coupled using a driving function, both the driver and the response system can be combined into one dynamical system[20-21]. The subscript 't' indicates the drive system and the subscript 'r' indicates the response system. The state variable 'a_R' in 'ϕ_R' and 'n_R' is replaced with 'a_T' to force the response system and synchronize it with the drive system. The corresponding non-linear differential equations that govern the drive and the response system are given below. These were modeled using MATLAB's DDE23 function.

Drive System:

$$\frac{da_T}{dt} = \frac{1}{2}\left[\frac{\gamma_c\gamma_n}{\gamma_s J} n_T - \gamma_p(2a_T + {a_T}^2)\right](1 + a_T) + \xi_i\gamma_c cos(\Omega t + \phi_T)$$

$$\frac{d\phi_T}{dt} = \frac{-b}{2}\left[\frac{\gamma_c\gamma_n}{\gamma_s J} n_T - \gamma_p(2a_T + {a_T}^2)\right](1 + a_T) - \frac{\xi_i\gamma_c}{1 + a_T} sin(\Omega t + \phi_T)$$

$$\frac{dn_T}{dt} = -\gamma_s n_T - \gamma_n(1 + a_T)^2 n_T - \gamma_s J(2a_T + {a_T}^2) + \frac{\gamma_s\gamma_p}{\gamma_c} J(2a_T + {a_T}^2)(1 + a_T)^2 + \xi_f\gamma_s(J + 1)(1 + a_T(t - \tau))^2$$

Response System:

$$\frac{da_R}{dt} = \frac{1}{2}\left[\frac{\gamma_c\gamma_n}{\gamma_s J} n_R - \gamma_p(2a_R + {a_R}^2)\right](1 + a_R) + \xi_i\gamma_c cos(\Omega t + \phi_R)$$

$$\frac{d\phi_R}{dt} = \frac{-b}{2}\left[\frac{\gamma_c\gamma_n}{\gamma_s J} n_R - \gamma_p(2a_T + {a_T}^2)\right](1 + a_T) - \frac{\xi_i\gamma_c}{1 + a_T} sin(\Omega t + \phi_R)$$

$$\frac{dn_R}{dt} = -\gamma_s n_R - \gamma_n(1 + a_T)^2 n_R - \gamma_s J(2a_T + {a_T}^2) + \frac{\gamma_s\gamma_p}{\gamma_c} J(2a_T + {a_T}^2)(1 + a_T)^2 + \xi_f\gamma_s(J + 1)(1 + a_T(t - \tau))^2$$

For simplicity, I am providing the illustration below to show how I modeled the aforementioned equations to successfully synchronize the radar network.

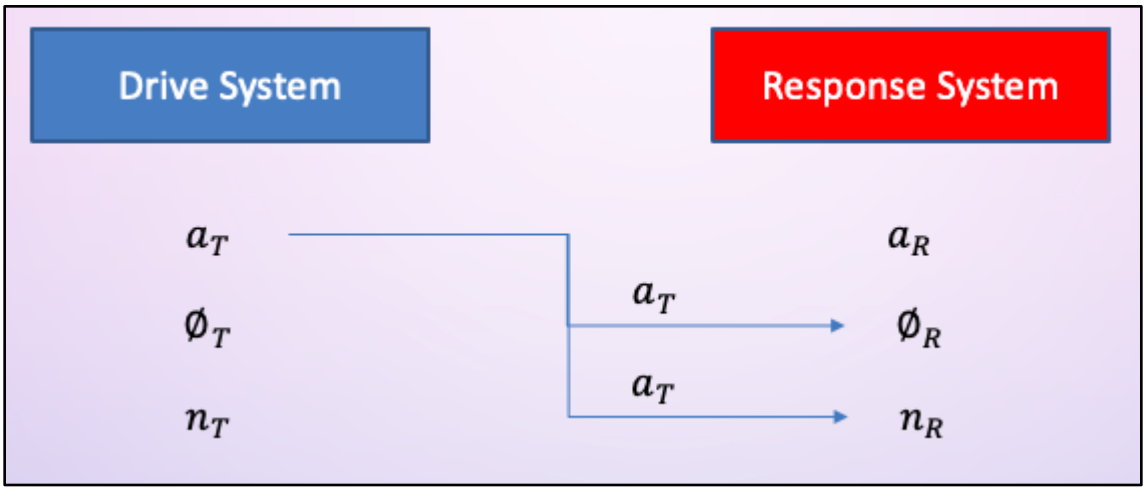

Figure 22: Illustration of radar network synchronization

There are various ways to see how our response system is synchronized. We will be discussing these methods in the next section.

6.3 Time-Series plot

For a synchronized radar network, we observe that the time-series behavior of the response system $a_R(t)$replicates the driver system $a_T(t)$(Fig. 23). However, when the system is not synchronized, the response and the drive system don't replicate each other (Fig.24).

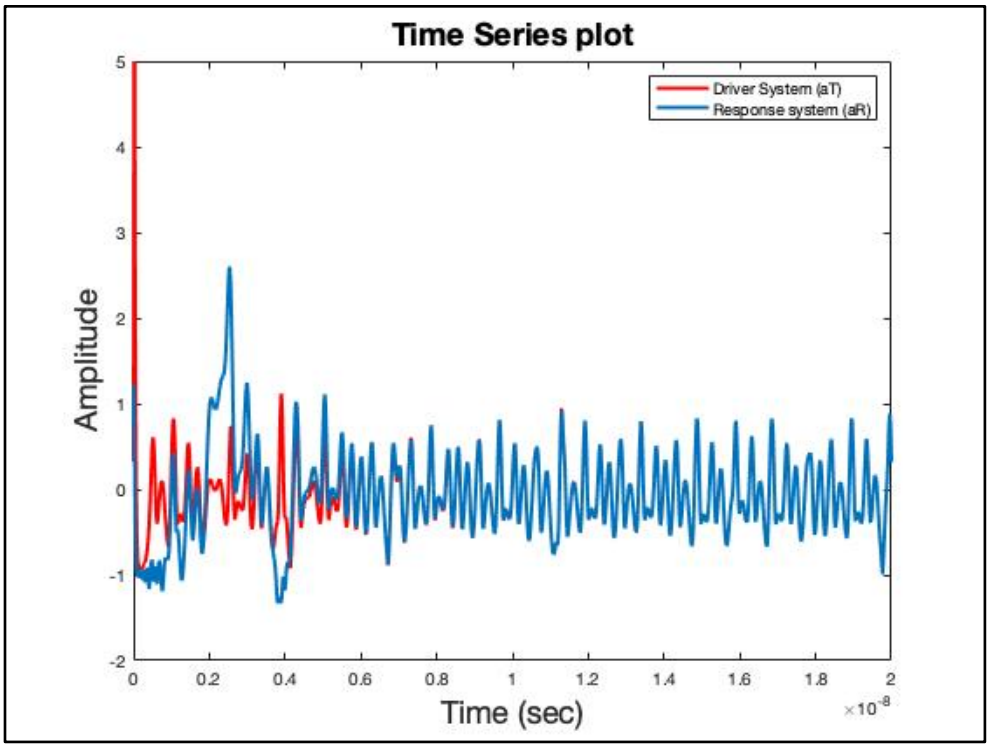

Figure 23: Time-Series plot for a synchronized system

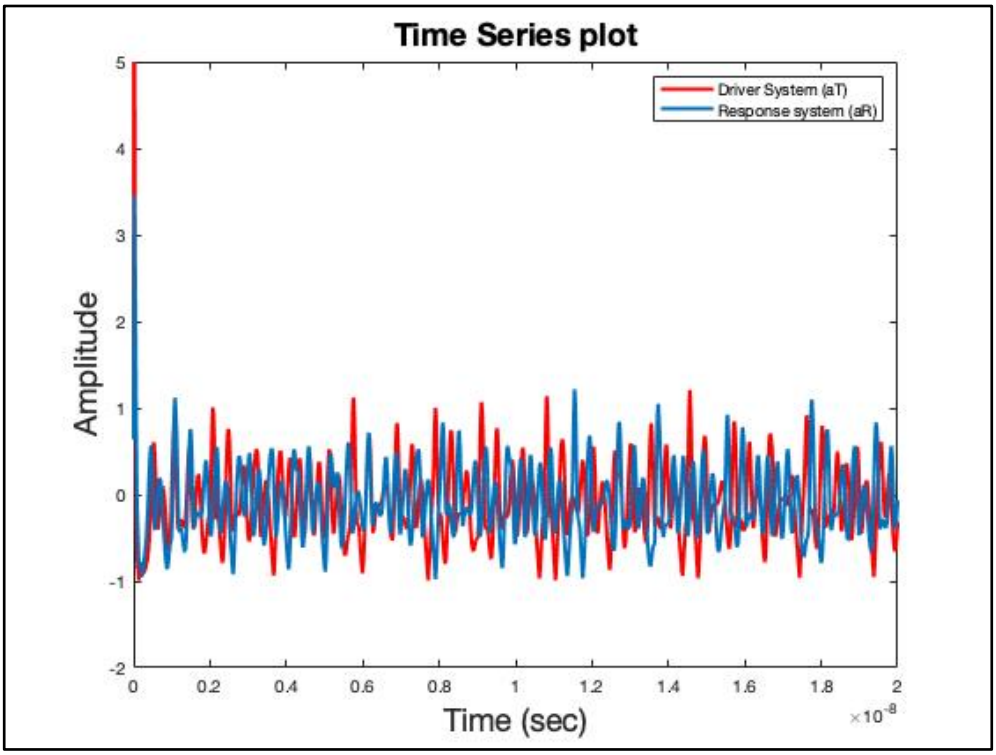

Figure 24: Time-series plot for an asynchronized system

6.4 Error Amplitude

When the system is synchronized, the error difference between our driver (a_T) and response waveform (a_R) , $|a_R - a_T|$is approaching zero asymptotically (Fig.25). Whereas, when our system is asynchronized, the error amplitude is very high and fluctuating arbitrarily(Fig.26).

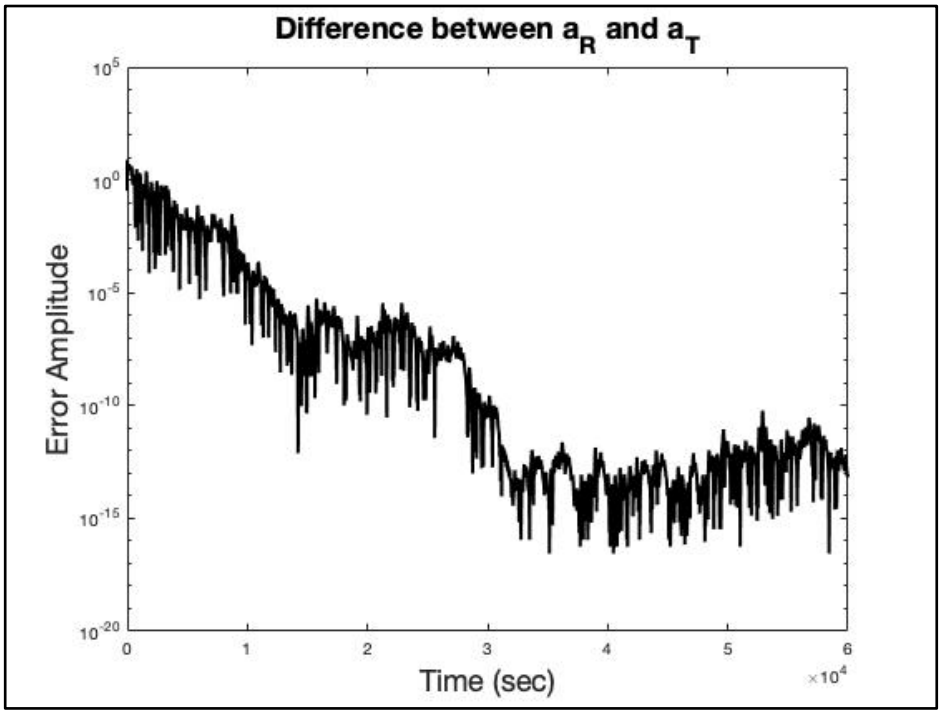

Figure 25: Error Amplitude for a synchronized system

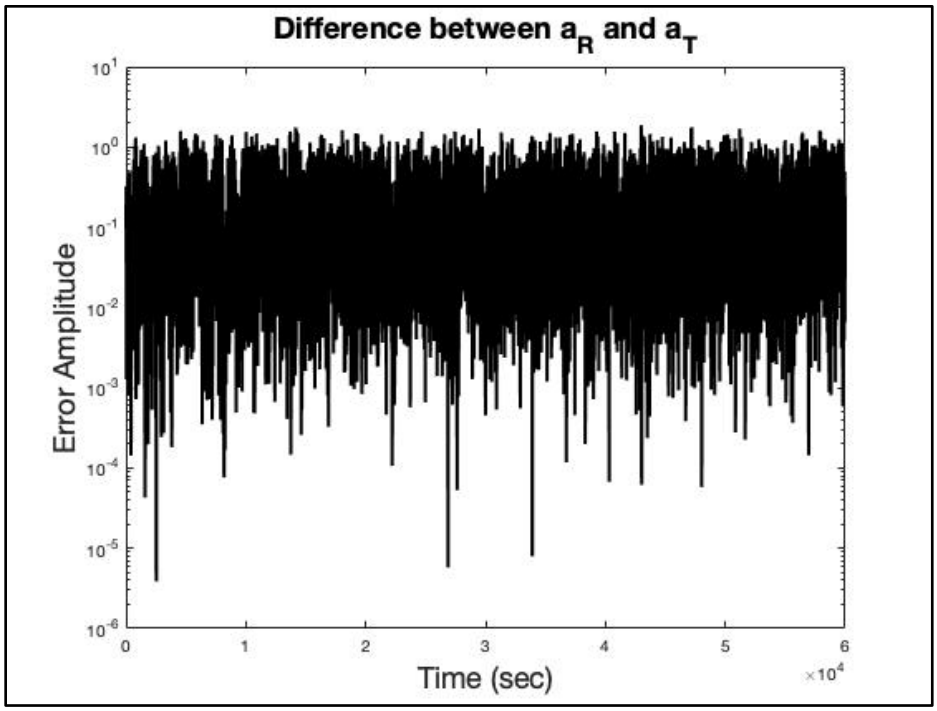

Figure 26: Error Amplitude for an asynchronized system

6.5 One-to-One plot

We obtain a linear plot between $a_R(t)$and $a_T(t)$showing that our system is synchronized and can be used for correlation analysis to detect targets (Fig.27). On the other hand, we do not get a linear plot for an asynchronized system (Fig.28). This shows us that this system cannot be used to detect targets.

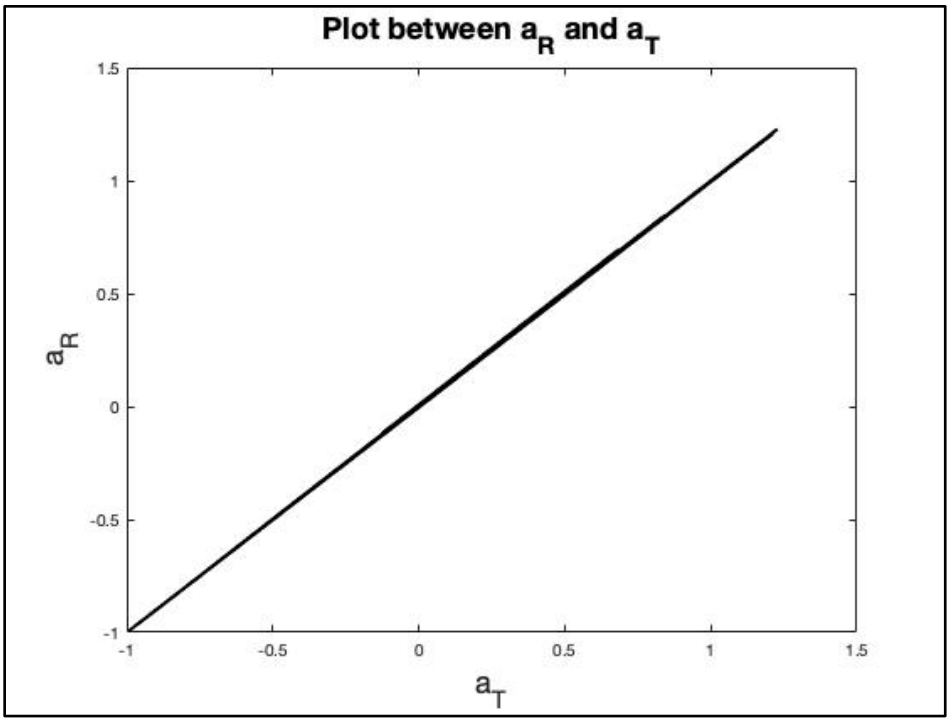

Figure 27: One-to-one plot for a synchronized system

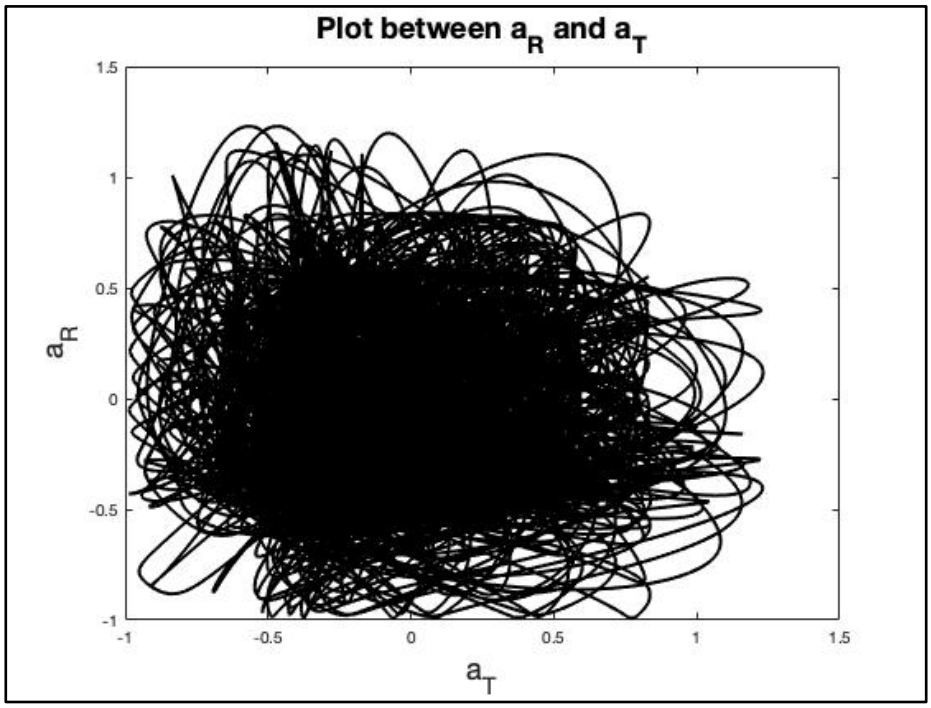

Figure 28: One-to-one plot for an asynchronized system

6.6 Correlation Analysis

We obtain a sharp correlation peak when the system is synchronized, which helps locate targets efficiently (Fig.29). When the system is not synchronized, the waveform has multiple oscillations and no main peak that could help obtain the target or its imagery (Fig.30).

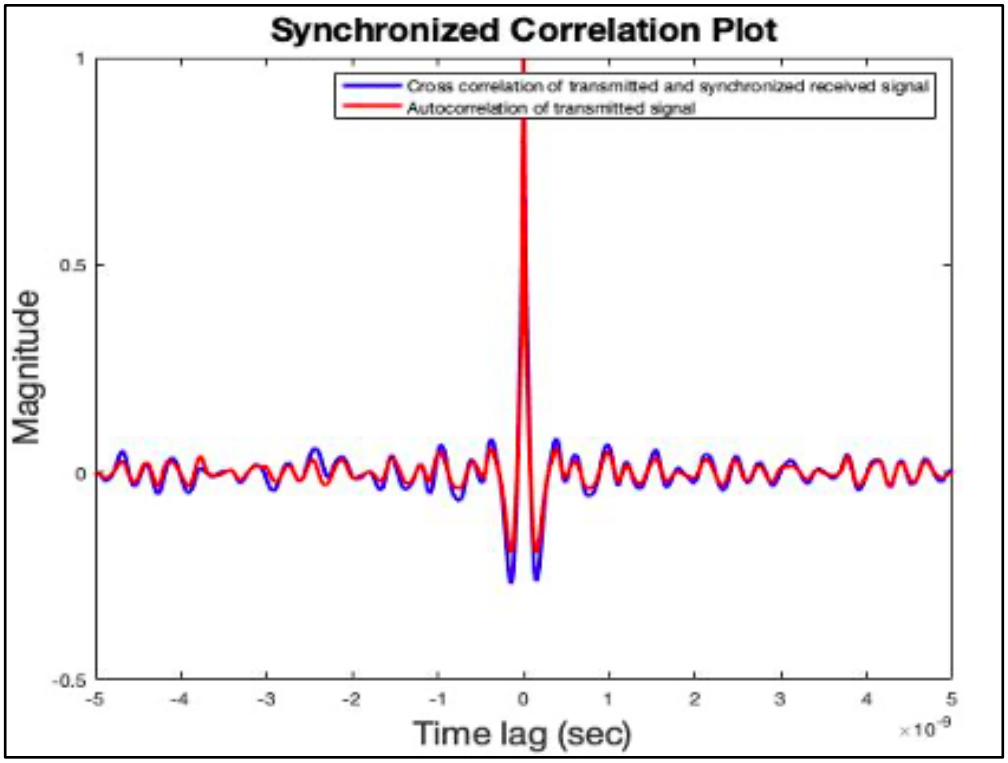

Figure 29: Correlation plot for a synchronized system

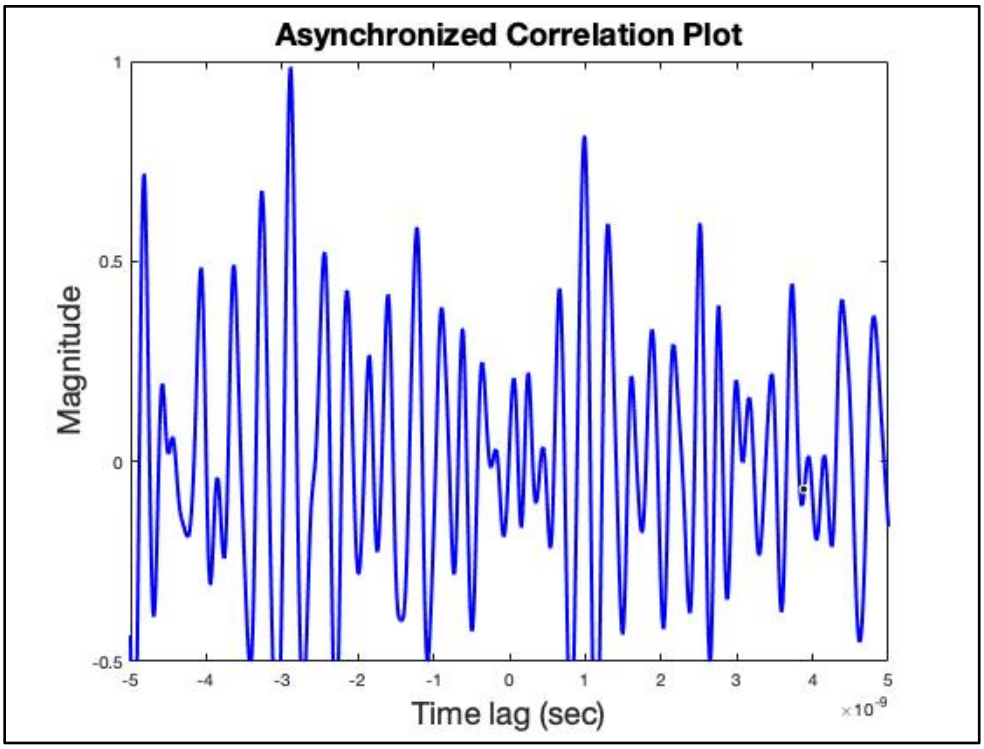

Figure 30: Correlation plot for an asynchronized system

6.7 Correlation Analysis using 'n' number of transceivers

In this section, we will show how a synchronized radar network can be synchronized using 'n' number of transmitter and receiver nodes and it would still give us persistent sharp correlation peaks. We will do a case-by-case synchronization for n=1,2,3, and 4, where n is the number of oscillators, to understand how correlation analysis helps detect targets efficiently using high-quality wideband chaotic signals.

Case 1:n=1

Here, we are considering the correlation of the transmitter with itself i.e the autocorrelation as the first oscillator. We used the top three equations mentioned in Section 6.2 to obtain the following plot:

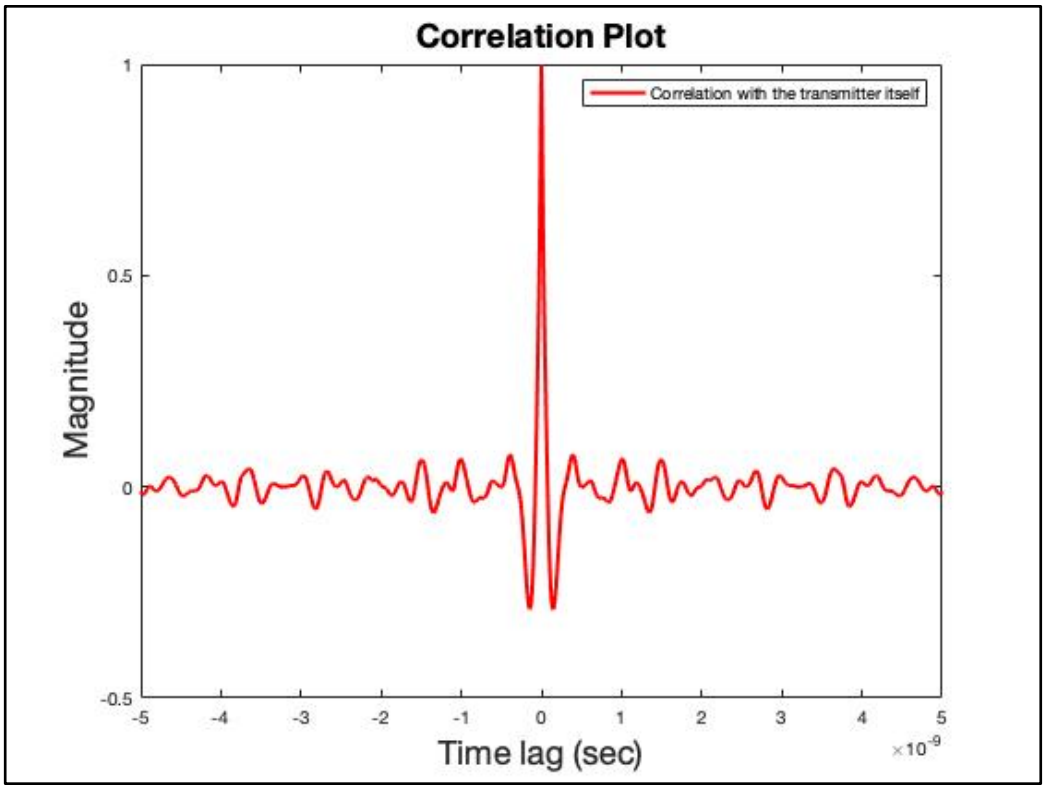

Figure 31: Correlation for n=1 i.e. one transmitter

Case 2: n=2

In this case, we assume that both oscillators are present at different locations. Any of the oscillators can transmit a waveform and the other at receiver can be used for the synchronization. Thus, we have a set of six equations and six different initial conditions. The equations are similar to those shown in section 7.2.

The echo received from the target is used to correlate with the synchronized waveform at the receiver. The cross correlation plot between the two oscillators, the transmitter and receiver, is shown below.

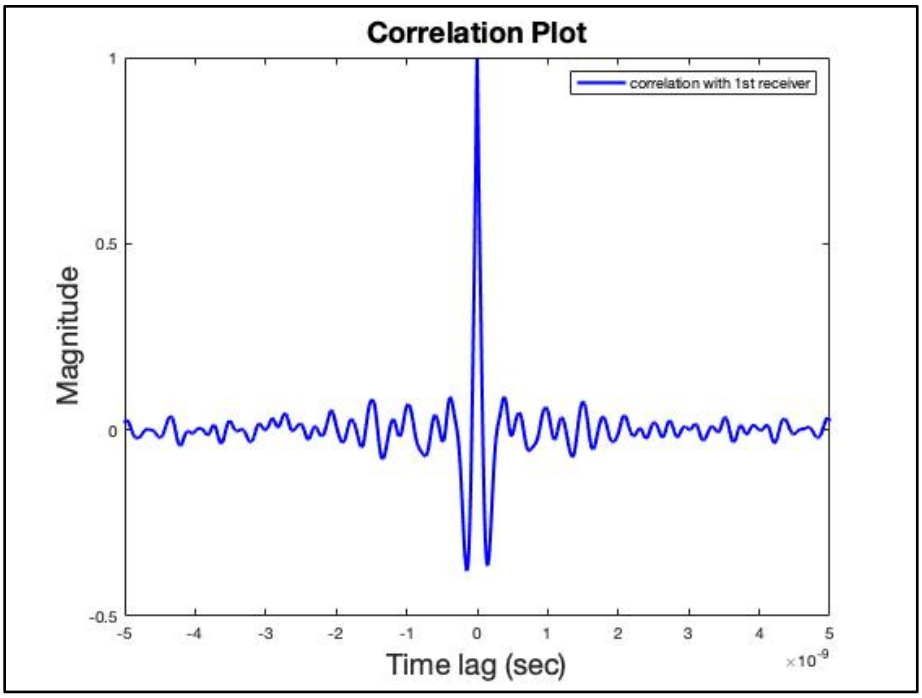

Figure 32: Cross correlation for n=2 i.e. two oscillators

Case 3: n=3

Now we consider three oscillators placed at different locations to see if we still obtain a sharp correlation peak. There is one transmitter and two receivers, and either of the oscillators can transmit a waveform while the others at the receiver can be used for synchronization. We used the following equations to model this case:

Drive System

$$\frac{da_T}{dt} = \frac{1}{2}\left[\frac{\gamma_c\gamma_n}{\gamma_s J} n_T - \gamma_p(2a_T + {a_T}^2)\right](1 + a_T) + \xi_i\gamma_c cos(\Omega t + \phi_T)$$

$$\frac{d\phi_T}{dt} = \frac{-b}{2}\left[\frac{\gamma_c\gamma_n}{\gamma_s J} n_T - \gamma_p(2a_T + {a_T}^2)\right](1 + a_T) - \frac{\xi_i\gamma_c}{1 + a_T} sin(\Omega t + \phi_T)$$

$$\frac{dn_T}{dt} = -\gamma_s n_T - \gamma_n(1 + a_T)^2 n_T - \gamma_s J(2a_T + {a_T}^2) + \frac{\gamma_s\gamma_p}{\gamma_c} J(2a_T + {a_T}^2)(1 + a_T)^2$$

$$+ \xi_f\gamma_s(J + 1)(1 + a_T(t - \tau))^2$$

Response System 1

$$\frac{da_R}{dt} = \frac{1}{2}\left[\frac{\gamma_c\gamma_n}{\gamma_s J} n_R - \gamma_p(2a_R + {a_R}^2)\right](1 + a_R) + \xi_i\gamma_c cos(\Omega t + \phi_R)$$

$$\frac{d\phi_R}{dt} = \frac{-b}{2}\left[\frac{\gamma_c\gamma_n}{\gamma_s J} n_R - \gamma_p(2a_T + {a_T}^2)\right](1 + a_T) - \frac{\xi_i\gamma_c}{1 + a_T} sin(\Omega t + \phi_R)$$

$$\frac{dn_R}{dt} = -\gamma_s n_R - \gamma_n(1 + a_T)^2 n_R - \gamma_s J(2a_T + {a_T}^2) + \frac{\gamma_s\gamma_p}{\gamma_c} J(2a_T + {a_T}^2)(1 + a_T)^2$$

$$+ \xi_f\gamma_s(J + 1)(1 + a_T(t - \tau))^2$$

Response System 2

$$\frac{da_R}{dt} = \frac{1}{2}\left[\frac{\gamma_c\gamma_n}{\gamma_s J} n_R - \gamma_p(2a_R + {a_R}^2)\right](1 + a_R) + \xi_i\gamma_c cos(\Omega t + \phi_R)$$

$$\frac{d\phi_R}{dt} = \frac{-b}{2}\left[\frac{\gamma_c\gamma_n}{\gamma_s J} n_R - \gamma_p(2a_T + {a_T}^2)\right](1 + a_T) - \frac{\xi_i\gamma_c}{1 + a_T} sin(\Omega t + \phi_R)$$

$$\frac{dn_R}{dt} = -\gamma_s n_R - \gamma_n(1 + a_T)^2 n_R - \gamma_s J(2a_T + {a_T}^2) + \frac{\gamma_s\gamma_p}{\gamma_c} J(2a_T + {a_T}^2)(1 + a_T)^2$$

$$+ \xi_f\gamma_s(J + 1)(1 + a_T(t - \tau))^2$$

We used a set of nine equations along with nine different initial conditions to obtain the cross correlation between the transmitter and receivers. The thing that makes this analysis efficient is that just by replacing the response variable $(a_R)$by the drive variable (a_T)in the response system equations, we can use either of the oscillators as synchronized receivers and the other as transmitter. This holds true for all the cases presented above and below too.

We obtained the following results for cross correlation using these equations:

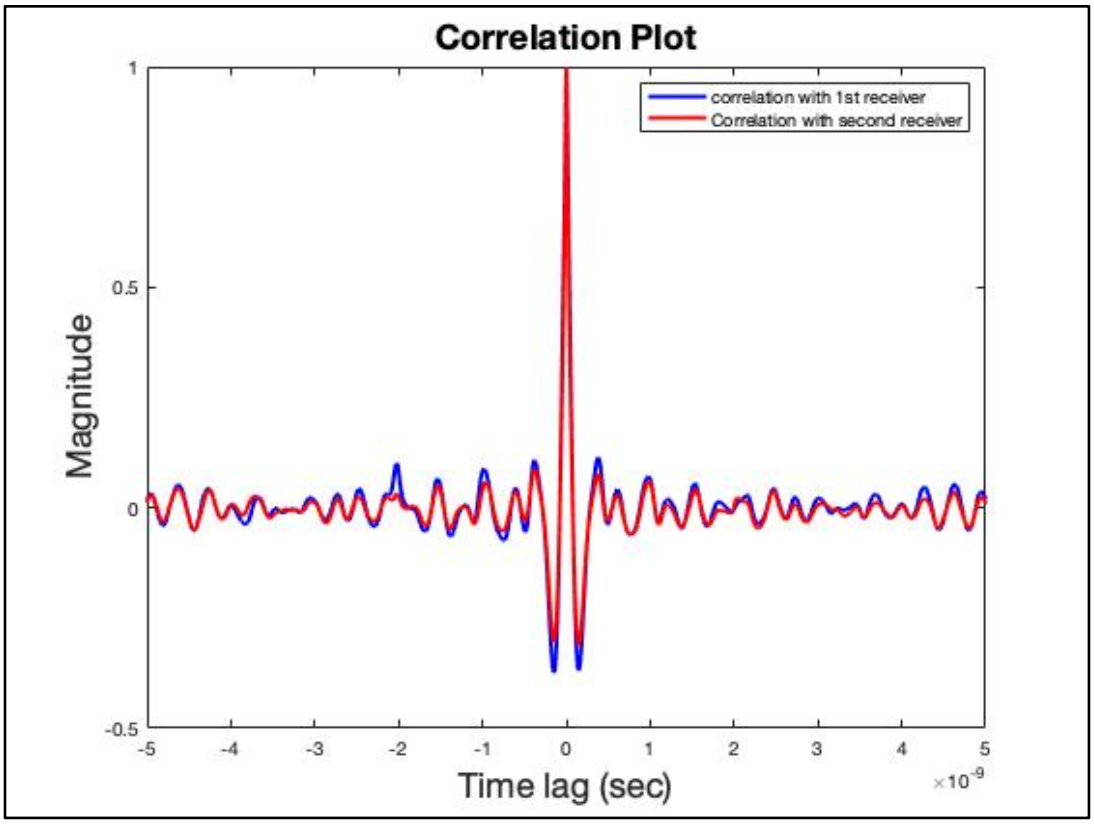

Figure 33: Cross Correlation for n=3 i.e. one transmitter and two receiver oscillators

Case 4: n=4

In this case, we assume that 4 oscillators (one transmitter and three receivers) are present at different locations. We use the following twelve equations with twelve different initial conditions to obtain the cross correlation of each receiver with the transmitter:

Drive System

$$\frac{da_T}{dt} = \frac{1}{2}\left[\frac{\gamma_c\gamma_n}{\gamma_s J} n_T - \gamma_p(2a_T + {a_T}^2)\right](1 + a_T) + \xi_i\gamma_c cos(\Omega t + \phi_T)$$

$$\frac{d\phi_T}{dt} = \frac{-b}{2}\left[\frac{\gamma_c\gamma_n}{\gamma_s J} n_T - \gamma_p(2a_T + {a_T}^2)\right](1 + a_T) - \frac{\xi_i\gamma_c}{1 + a_T} sin(\Omega t + \phi_T)$$

$$\frac{dn_T}{dt} = -\gamma_s n_T - \gamma_n(1 + a_T)^2 n_T - \gamma_s J(2a_T + {a_T}^2) + \frac{\gamma_s\gamma_p}{\gamma_c} J(2a_T + {a_T}^2)(1 + a_T)^2$$

$$+ \xi_f\gamma_s(J + 1)(1 + a_T(t - \tau))^2$$

Response System 1

$$\frac{da_R}{dt} = \frac{1}{2}\left[\frac{\gamma_c\gamma_n}{\gamma_s J}n_R - \gamma_p(2a_R + {a_R}^2)\right](1 + a_R) + \xi_i\gamma_c cos(\Omega t + \phi_R)$$

$$\frac{d\phi_R}{dt} = \frac{-b}{2}\left[\frac{\gamma_c\gamma_n}{\gamma_s J}n_R - \gamma_p(2a_T + {a_T}^2)\right](1 + a_T) - \frac{\xi_i\gamma_c}{1 + a_T}sin(\Omega t + \phi_R)$$

$$\frac{dn_R}{dt} = -\gamma_s n_R - \gamma_n(1 + a_T)^2 n_R - \gamma_s J(2a_T + {a_T}^2) + \frac{\gamma_s\gamma_p}{\gamma_c}J(2a_T + {a_T}^2)(1 + a_T)^2$$

$$+ \xi_f\gamma_s(J + 1)(1 + a_T(t - \tau))^2$$

Response System 2

$$\frac{da_{R1}}{dt} = \frac{1}{2}\left[\frac{\gamma_c\gamma_n}{\gamma_s J}n_{R1} - \gamma_p(2a_{R1} + {a_{R1}}^2)\right](1 + a_{R1}) + \xi_i\gamma_c cos(\Omega t + \phi_{R1})$$

$$\frac{d\phi_{R1}}{dt} = \frac{-b}{2}\left[\frac{\gamma_c\gamma_n}{\gamma_s J}n_{R1} - \gamma_p(2a_T + {a_T}^2)\right](1 + a_T) - \frac{\xi_i\gamma_c}{1 + a_T}sin(\Omega t + \phi_{R1})$$

$$\frac{dn_{R1}}{dt} = -\gamma_s n_{R1} - \gamma_n(1 + a_T)^2 n_{R1} - \gamma_s J(2a_T + {a_T}^2) + \frac{\gamma_s\gamma_p}{\gamma_c}J(2a_T + {a_T}^2)(1 + a_T)^2$$

$$+ \xi_f\gamma_s(J + 1)(1 + a_T(t - \tau))^2$$

Response System 3

$$\frac{da_{R2}}{dt} = \frac{1}{2}\left[\frac{\gamma_c\gamma_n}{\gamma_s J}n_{R2} - \gamma_p(2a_{R2} + {a_{R2}}^2)\right](1 + a_{R2}) + \xi_i\gamma_c cos(\Omega t + \phi_{R2})$$

$$\frac{d\phi_{R2}}{dt} = \frac{-b}{2}\left[\frac{\gamma_c\gamma_n}{\gamma_s J}n_{R2} - \gamma_p(2a_T + {a_T}^2)\right](1 + a_T) - \frac{\xi_i\gamma_c}{1 + a_T}sin(\Omega t + \phi_{R2})$$

$$\frac{dn_{R2}}{dt} = -\gamma_s n_{R2} - \gamma_n(1 + a_T)^2 n_{R2} - \gamma_s J(2a_T + {a_T}^2) + \frac{\gamma_s\gamma_p}{\gamma_c}J(2a_T + {a_T}^2)(1 + a_T)^2$$

$$+ \xi_f\gamma_s(J + 1)(1 + a_T(t - \tau))^2$$

Either of the oscillators can be used as a transmitter or a synchronized receiver by replacing the response variable by the drive variable. We obtained the following plot for this case:

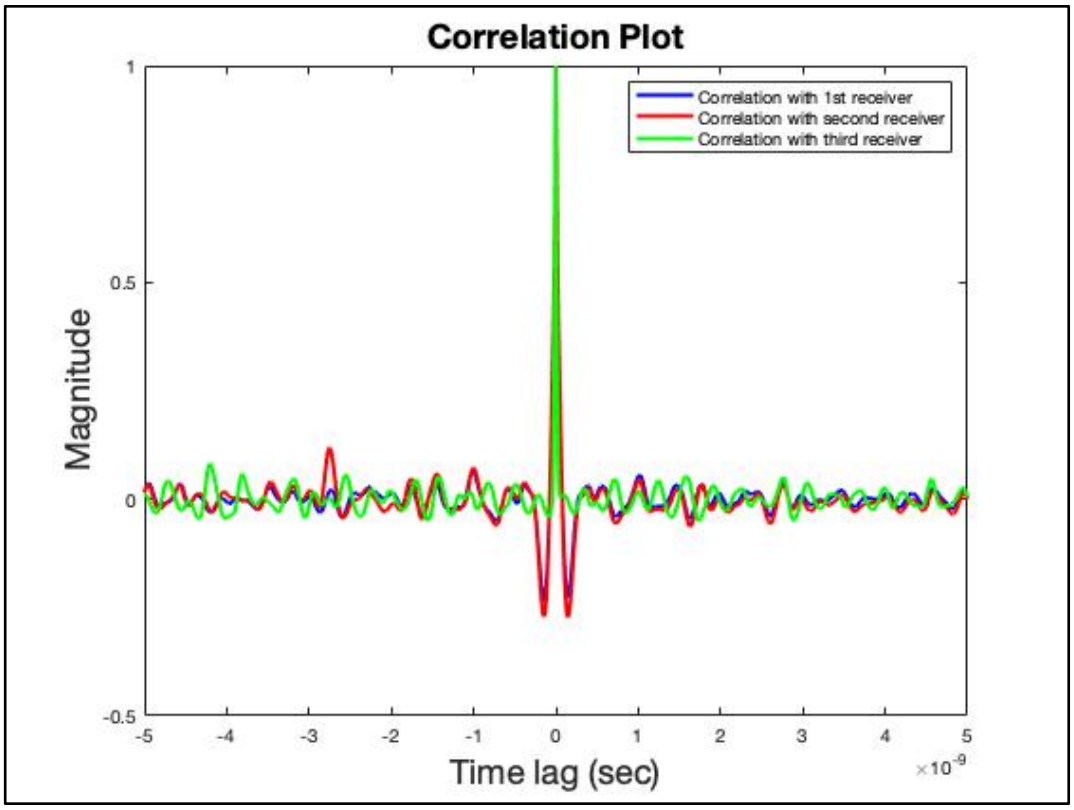

Figure 34: Cross Correlation for n=4 i.e. three receiver oscillators and one transmitter

As we can see from Fig.31,32,33, and 34, we obtain sharp correlation peaks with dying out sidelobes indicating the location of the target. Now, we will run the same analysis for two-point target simulations with all four oscillators, assuming they are present at different locations. This will help us observe if we get two sharp correlation peaks indicating the presence of the targets when we do the cross correlation. Each of the synchronized receivers are being correlated with the received signal from the two-point target simulation.

Case 1: First Synchronized Receiver

We are using the equations shown in the section above for case n=4. We obtain the following cross correlation plot between the first synchronized receiver and the received signal from the two-point target simulation:

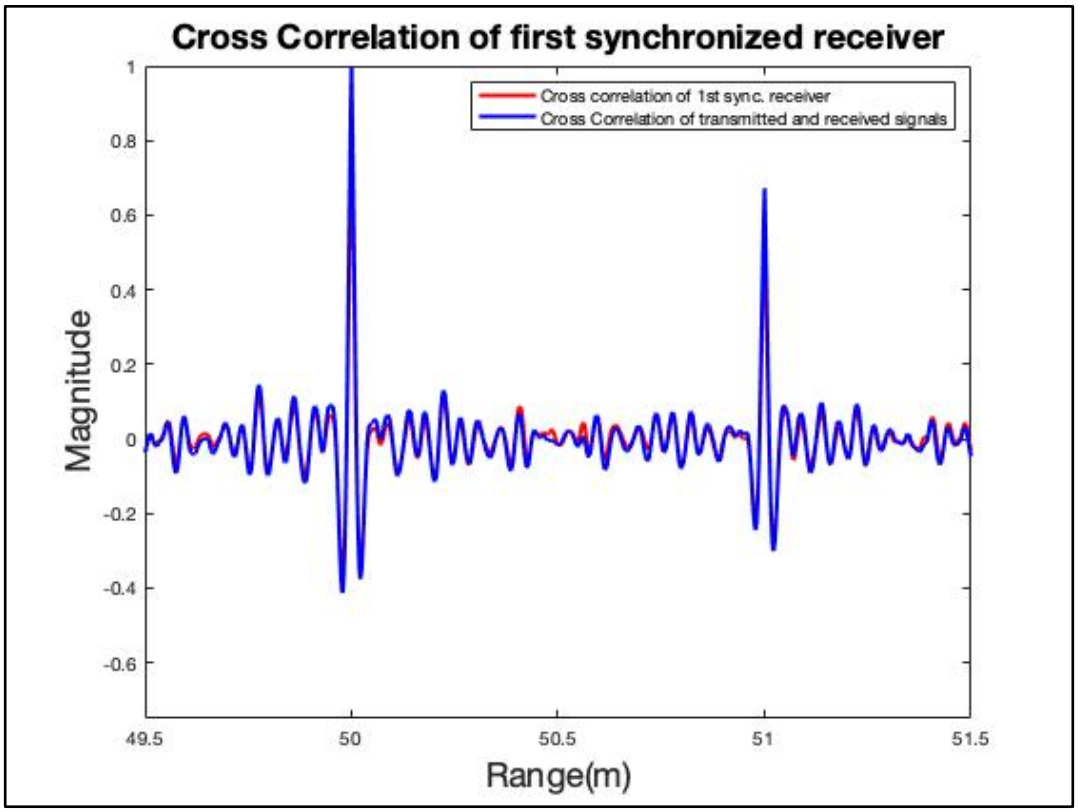

Figure 35: Two-point target simulation with two oscillators

Case 2: Second Synchronized Receiver

In this case, we ran our simulation for obtaining the cross correlation plot between the second synchronized receiver and the received signal from the two-point target simulation:

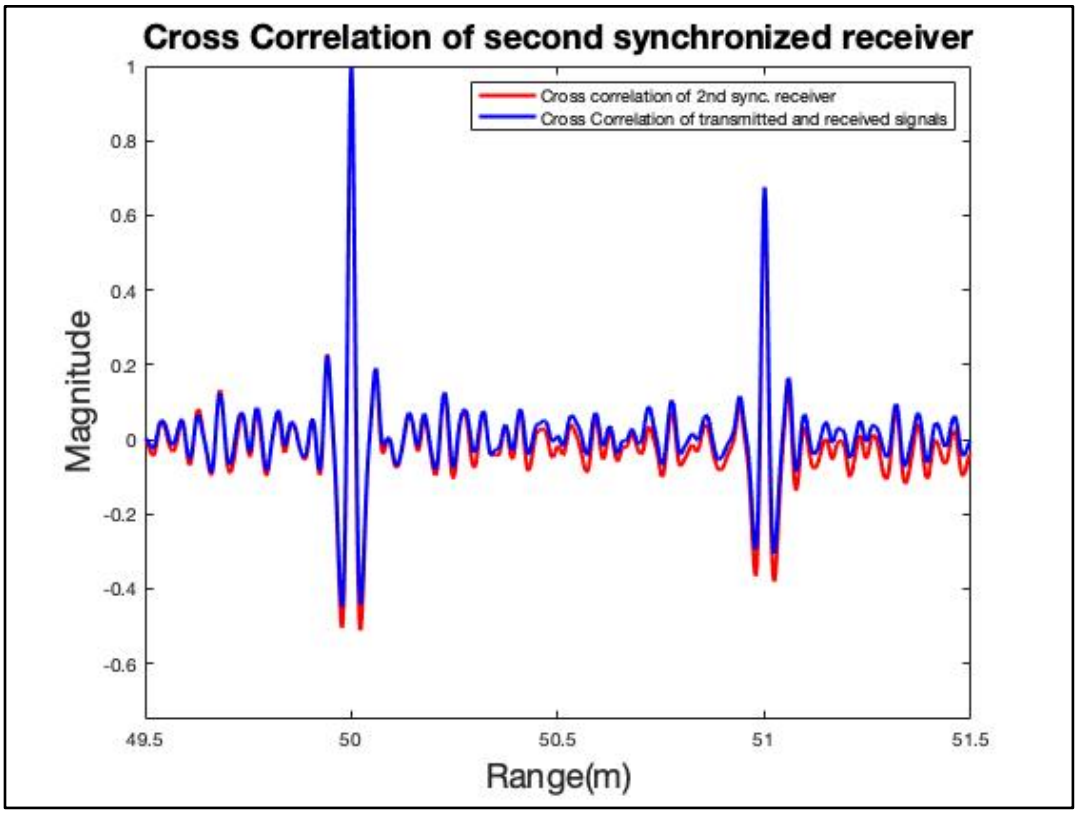

Figure 36: Two-point target simulation with three oscillators

Case 3: Third Synchronized Receiver

Lastly, we obtain the cross-correlation plot between the third synchronized receiver and the received signal from the two-point target simulation. This is shown below:

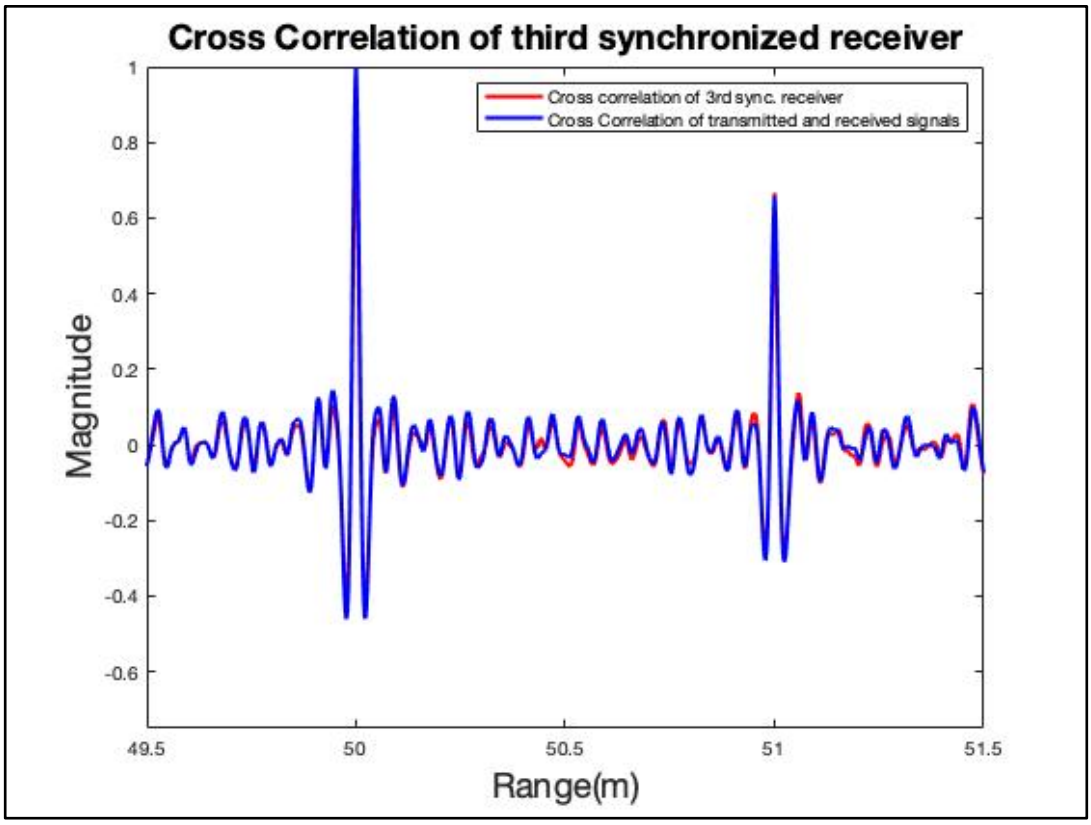

Figure 37: Two point target simulation with three receiver oscillators and one transmitter

As we can see from Fig.35,36, and 37, we obtain two sharp correlation peaks at R1=50m and R2=51m indicating the presence of two targets separated by a distance of 1m. If we recall from section 6.2, that is where we had placed our targets. This testing shows that a synchronized radar network with 'n' number of transceivers can help detect targets efficiently and accurately.

7. Performance Estimates and Results

In the previous sections, I have already discussed the drawbacks of previous chaotic systems we studied and how we chose our final design i.e. the Lang-Kobayashi system (Section 4). I also discussed the testing results for choosing the most efficient semiconductor laser system amongst three of them (Section 5). Henceforth, in this section I will provide an overview of everything we have discussed so far in this report.

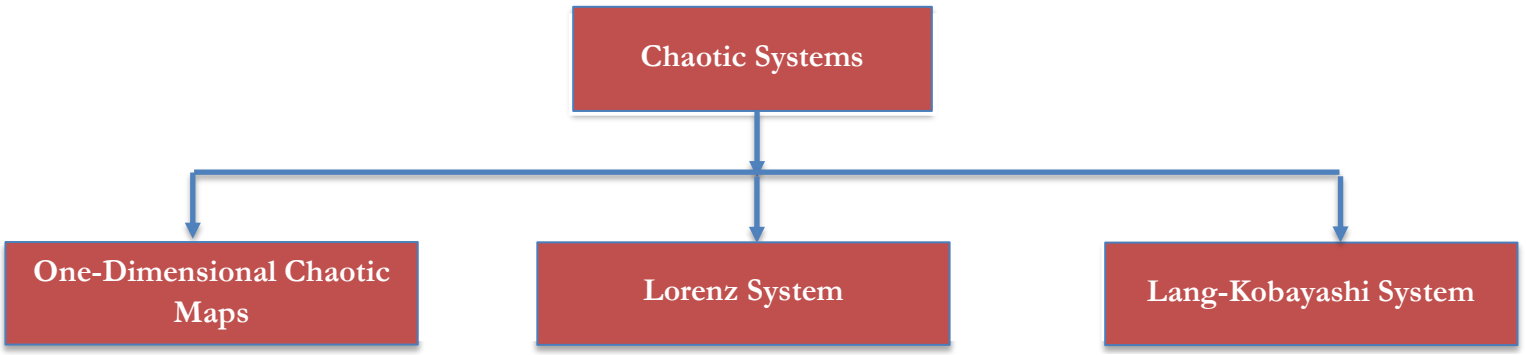

- Uses single waveforms instead of multiple waveforms.
- Displays chaotic behavior in response to the change in control parameters of the equations.
- Makes the process of signal transmission difficult.
- Unable to generate wideband chaotic signals due to the aforementioned drawbacks

- Depicts chaotic behavior using multiple waveforms.
- Sensitive to initial conditions.
- Estimated to produce wideband chaotic signals but oscillates at lower frequencies.
- Requires additional hardware to oscillate at higher frequencies.
- Additional hardware implies increased degree of clutter and noise, which is undesirable for radar imaging.
- Couldn't be used to detect targets due to the aforementioned drawbacks.

- Shows highly chaotic behavior using delay differential equations.
- Sensitive to initial conditions.
- Estimated to produce wideband chaotic signals and it does.
- Generated using OI scheme, which is a type of semiconductor laser system.
- Helps obtain a flat and wideband spectrum desirable for radar imaging.
- Synchronized to detect targets efficiently.

8. Production Schedule

This research project required an immense amount of work in terms of studying various chaotic systems mathematically and implementing them in MATLAB. Thus, we made the following schedule to accomplish all the tasks required to obtain the final design of the synchronized radar network.

Table 6: Production and implementation schedule of the design project

Research Subject	Capstone Subject	Timeline
One-dimensional chaotic maps	Research	January-March 2020
Lorenz System	Research and Design	June 2020
Lang-Kobayashi System	Research and Design	June-August 2020
Spectrum and Autocorrelation of the transmitted signal of Lang-Kobayashi system	Research and Compute; Prepare ECE-498 presentation; Prepare the project report	September-November 2020
Two-point Target simulation	Simulate and Research	November-December 2020
Radar Network Synchronization and Correlational Analysis	Simulate, Research, Implement as final design of the system	December-February 2021
Testing with different semiconductor laser chaotic systems	Testing the final design; Prepare ECE-499 presentation; Prepare the final project report	February-March 2021
Ambiguity function analysis and Radar Target Imaging	Future work	April-June 2021(to be continued)

There were times when software simulations required more time than we had estimated, but we tried our best to stick to our schedule. This project was all based on software, but it took a lot of efforts to reach our goal of synchronizing the radar network and detecting targets efficiently. It required learning different techniques and metrics pertaining to the field of radar imaging and also

experimenting with different MATLAB functions to see how we can make it easy for a user to test our system. I also had to learn how to solve and model delay differential equations in MATLAB before modeling the Lang-Kobayashi system. It was very tough to debug code at every step while ensuring the functionality of the radar network. At last, I can proudly say that under continuous guidance of my advisor, I was able to achieve the results we aimed for.

9. Cost Analysis

We did all our simulations on software so we did not incur any costs for this project. However, it is important to provide a market-based cost analysis for hardware components that can be bought to prototype and test the system. Our goal was to replace hardware components and theoretically present the software simulation results. We can validate our results by purchasing equipment and comparing the results a hardware and a software system yields.

In case one wants to replicate our research or test it out, they would require the MATLAB software, which can be easily downloaded from [28] and is free of cost.

Table 7: Cost Analysis of hardware components based on market research

Hardware Component	Quantity needed	Cost
InGaAs Photodetector [22]	3	$5.50-$92.0/piece
Tektronix TDS694C Oscilloscope (3GHz bandwidth and 10GS/s sampling rate) [23]	1	$2750/piece
HP E4407B spectrum analyzer (26.5 GHz bandwidth) [24]	1	$4600/piece
Picosecond Pulse Labs 5100 Broadband Pulse Inverter [24]	1	$719.95/piece
InGaAsP–InP single-mode DFB lasers (master and slave lasers) [24]	6	$40-$120/piece

Two-stage Avantek SSF886 amplifiers [24]	2	$89.95/piece

These components are mainly used to prototype the semiconductor laser systems and are very expensive. This is not an exhaustive list of all the components needed but mainly can be used to design the hardware system to test and generate signals.

10. User Manual

This section provides detailed instructions on how to generate, implement, and test the system. It is assumed that the user has the MATLAB software downloaded on their computer.

Setup:

1) First step is to ensure that the user has access to all the documents we referred to for modeling delay differential equations, values of control parameters that were used in various equations, and the theory that describes how semiconductor laser systems work.
2) Second step is to set up MATLAB and know how to run the coded program on it. We use the following icon:

Operation:

1) The user needs to just run the program to understand how the radar network synchronization works, assuming that the transmitter and receivers are present at different locations.
2) Second step is to know the frequency band in which our system can operate i.e. 10-15 GHz so that they can ensure we are not violating any IEEE standards. Once they run the program to obtain Power Spectral Density, they will observe that our frequency ranges from 0-10 GHz.
3) The way the synchronization has been set up in MATLAB, the user will have to press 0 to see synchronization results and press 1 to see the results for an asynchronized system. When the user runs the program, they will be prompted to "Press a key:", and after pressing a key they can see the results. Refer to the snapshot below:

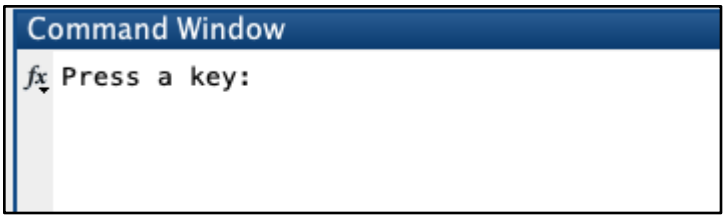

4) To compute mathematical expressions like range resolution or mainlobe width, the user can zoom into the plot and calculate the metrics to verify theoretical and experimental results. They can zoom in/out using the following icon:

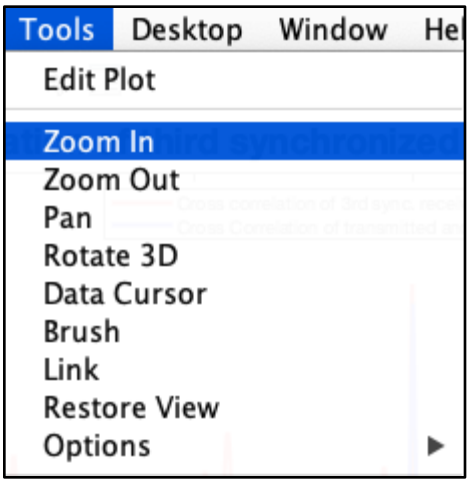

5) If the user wants to validate the location of targets, they will have to observe sharp correlation peaks in the cross correlation plots because that is what indicates the presence of targets.

6) In case the user wants to play around with the radar network synchronization using 'n' number of oscillators, they can do so by referring to the equations and methodology given in this report in Section 6. They will also need to understand the metrics that help compare a synchronized and an asynchronized system so that they know what the different plots signify.

Troubleshooting:

1) This project and all the simulations are on MATLAB. All the code has been verified so there should be no problem while running the system. Although, in case a user does not know

how to work with MATLAB, we can provide the basic guidelines that explain the working of the software.

2) In case a section of code does not work, the user can document it for us so that we can rectify the problem.
3) In case MATLAB stops working, just pause the program you are currently working on and quit the software. Then, restart the program. Sometimes, due to excessive code files, the program can slow down or even take a lot of time to generate plots. One can pause the program using the following icon:

Maintenance:

1) In terms of storage and maintenance, all the code will be documented for the user with appropriate file names. It is the user's responsibility to not amend the code or change any file names. This would lead to things not being documented properly if various users want to test the system out.
2) After the user has tested the program, they can either choose to keep MATLAB for future purposes or simply uninstall it.
3) If the user wishes to buy the hardware components to test this system out, they will have to ensure what their budget is and if they can store the hardware appropriately in their respective labs. All the equipment should be used after reading their datasheets because if not used properly, they could malfunction or corrupt the system.

11. Discussion, Conclusion, and Recommendations

11.1 Discussion

The problem of obtaining high-resolution radar imaging using traditional radar networks has been investigated by various researchers. A wide bandwidth waveform transmission is necessary to achieve high-resolution imaging of radar targets. In this research, we propose the potential of using semiconductor laser systems to generate wideband chaotic signals so that we can replace additional hardware. This would also reduce the clutter and noise our system might encounter. Additionally, the subject of synchronizing radar networks is gaining significant attention. This is because radar network synchronization helps detect targets efficiently and also filters out noise so that our system is not vulnerable to any kind of interference. Hence, in this research, we provide the final design of a synchronized multistatic radar network that can be used to detect multiple targets in close proximity.

11.2 Conclusion

This report presents the synchronization of a multistatic radar network and how it can be used to detect targets to obtain their high-resolution imagery. We considered the Lorenz chaotic system and implemented it using MATLAB functions to assess the frequency at which it oscillates, and if it helps detect targets. This chaotic system depicted low frequency oscillations and required additional hardware to generate wideband chaotic signals that can be used to detect targets and obtain their imagery. Hence, we proposed the Lang-Kobayashi system which is generated using the Optical Injection scheme, which is a type of semiconductor laser system. It utilizes the self-synchronization property of chaos and generates wideband chaotic signals that oscillate at higher frequencies (in the order of GHz). It also replaces additional hardware and gives better results in terms of radar network synchronization. We showed that this synchronization done using a

multistatic radar helps detect multiple targets in close proximity using high-quality signals. It also extracts additional information about the targets, such as their size and shape.

We found that the spectrum of this system is flat and wideband, which is desirable for our radar system. The frequency is in the range of 0-10 GHz, which shows that we were able to generate a wideband spectrum. The autocorrelation of the transmitted signal of our Lang-Kobayashi system gives a sharp peak with minimum sidelobes, indicating the location of the target. The main-lobe width is observed to be 0.13ns, which consequently gave a range resolution of 2cm. This helped us detect targets separated by a distance greater than 2cm. The cross-correlation of the synchronized and transmitted waveforms were of high-quality because they generated sharp correlation peaks indicating the presence of radar targets. The targets were separated by a distance of 1m, which is greater than 2cm. This validated our computation of range resolution and depicted enhanced detection capability of our system.

In the near future, we plan to study ambiguity functions of transmitted signals and analyze how they can be used to detect radar targets efficiently. Considering a complex target, we will generate high-resolution imagery of radar targets by synchronizing a multistatic radar network. Additionally, we will use image analysis metrics such as entropy, ambiguity function volume, etc. Lastly, we will evaluate the effects of noise and interference on imagery of the targets.

11.3 Lessons Learned and Recommendations

This project is completely functional but there are various lessons that were learned. Firstly, it was and is very important to document and comment the code so that we know what each line of code means. It is also important to study the mathematical delay differential or ordinary differential equations well in advance to model those in MATLAB. The biggest lesson I learned while working on this project was how to work independently and find answers yourself if you get stuck while

coding or are obtaining incorrect results. It took me a lot of time to code each task of our project and it required a lot of dedication and research to understand all of the radar terminology and mathematical concepts.

Few recommendations based on this project are that if someone wishes to validate our results using hardware components, they need to understand how each equipment works and shall have the budget to afford the equipment. Although our research is based completely on software, there are various ways in which we can improve the efficiency of our system by organizing the code more and making sure it is well-documented for a user to test it out. Lastly, this project required consistency in terms of working every day on it so that we do not fall behind in obtaining the required results. Sometimes, due to heavy terms, it was hard to work every day on it but if I had dedicated more time to it, we would have accomplished more. Thus, it is always recommended to stick to the project schedule and follow it religiously.

12. References

[1] H. D. Griffiths, "From a different perspective: principles, practice, and potential of bistatic radar," 2003 Proceedings of the International Conference on Radar (IEEE Cat. No.03EX695), Adelaide, SA, Australia, 2003, pp. 1-7, DOI: 10.1109/RADAR.2003.1278701.

[2] H. D. Griffiths, "New directions in bistatic radar," 2008 IEEE Radar Conference, Rome, Italy, 2008, pp. 1-6, DOI: 10.1109/RADAR.2008.4720719.

[3] M. Weib, "Synchronization of bistatic radar systems," IGARSS 2004. 2004 IEEE International Geoscience and Remote Sensing Symposium, Anchorage, AK, USA, 2004, pp. 1750-1753 vol.3, DOI: 10.1109/IGARSS.2004.1370671.

[4] Fan-Yi Lin and Jia-Ming Liu, "Diverse waveform generation using semiconductor lasers for radar and microwave applications," in *IEEE Journal of Quantum Electronics*, vol. 40, no. 6, pp. 682-689, June 2004, doi:10.1109/JQE.2004.828254.

[5] Y. Nijsure, G. Kaddoum and H. Leung, "Cognitive Chaotic UWB-MIMO Radar Based on Nonparametric BasedTechnique," IEEE Trans. Aerospace and Electronic Systems: 44(3), pp. 1240-1248, 2015.

[6] M. S. Willsey, K. V. Cuomo, and A. V. Oppenheim, "Quasi-Orthogonal Wideband Radar Waveforms Based on Chaotic Systems," IEEE Trans. Aerospace and Electronic Systems: 47(3), pp. 1974-1984, 2010.

[7] C. Cheng, Y. Chen AND F. Lin, "Generation of Uncorrelated Multichannel Chaos by Electrical Heterodyning for Multiple-Input– Multiple-Output Chaos Radar Application," in *IEEE Photonics Journal*, vol. 8, no. 1, pp. 1-14, Feb. 2016, Art no. 7800209, DOI: 10.1109/JPHOT.2015.2510327.

[8] Fan-Yi Lin and Jia-Ming Liu, "Chaotic Radar Using Nonlinear Laser Dynamics," in *IEEE Journal of QuantumElectronics*, vol. 40, no. 6, pp. 815-820, June 2004, DOI: 10.1109/JQE.2004.828237.

[9] Wolff, Christian." Radar Basics - MIMO Radar", Online, https://www.radartutorial.eu/02.basics/MIMO-radar.en.html

[10] B. C. Flores, E. A. Solis, and G. Thomas, "Assessment of Chaos-based FM Signals for Range-DopplerImaging," Proc. IEEE Radar, Sonar and Navigation: 150(4), pp. 312-322, 2003.

[11] M. Mandlik and Z. Nemec, "An accuracy synchronization method for passive radar system," 2014 24th International Conference Radioelektronika, Bratislava, Slovakia, 2014, pp. 1-4, doi: 10.1109/Radioelek.2014.6828480.

[12] "IEEE Standard Letter Designations for Radar-Frequency Bands," in IEEE Std 521-2019 (Revision of IEEE Std 521-2002), vol., no., pp.1-15, 14 Feb. 2020, doi: 10.1109/IEEESTD.2020.8999849.

[13] "IEEE Standard for Radar Definitions," in IEEE Std 686-2017 (Revision of IEEE Std 686- 2008), vol., no., pp.1-54, 13Sept. 2017, doi: 10.1109/IEEESTD.2017.8048479.

[14] "IEEE Standard for Software and System Test Documentation," in IEEE Std 829-2008, vol., no., pp.1-150, 18 July2008, doi: 10.1109/IEEESTD.2008.4578383.

[15] "Chaos Theory." *Encyclopedia Britannica*, Encyclopedia Britannica, Inc., 25 Sept. 2020,www.britannica.com/science/chaos-theory.

[16] "The Logistic Map." *Complexity Explorables*, 30 Apr. 2018, www.complexity-explorables.org/flongs/logistic/.

[17] Chih-Hao Cheng, Yi-Cheng Chen, and Fan-Yi Lin, "Chaos time delay signature suppression and bandwidth enhancement by electrical heterodyning," Opt. Express 23, 2308-2319 (2015)

[18] "RF Wireless World." *Radar Range | Radar Range Resolution*, www.rfwireless-world.com/Tutorials/radar-range-vs-range-resolution.html.

[19] L. M. Pecora and T. L. Carroll,Synchronization in chaotic systems, *Phys. Rev. Lett.*, vol. 64, no. 8, pp. 821–824, Feb. 1990.

[20] L. M. Pecora, and T. L. Carroll, Driving systems with chaotic signals, *Phys. Rev. A*, vol. 44, no. 4, pp. 2374–2383, Aug. 1991.

[21] "Find Quality Manufacturers, Suppliers, Exporters, Importers, Buyers, Wholesalers, Products and Trade Leads from Our Award-Winning International Trade Site. Import & Export on Alibaba.com." *Alibaba*, www.alibaba.com/.

[22]"TekTronix-TDS694C", www.ebay.com/sch/i.html?_from=R40&_trksid=p2380057.m570.l1312&_nkw=tektronix%2Btds694c&_sacat=181995.

[23] "Electronics, Cars, Fashion, Collectibles & More." *EBay*, www.ebay.com/.

[24] TL;, Carroll. "Chaotic System for Self-Synchronizing Doppler Measurement." *Chaos (Woodbury, N.Y.)*, U.S. National Library of Medicine, pubmed.ncbi.nlm.nih.gov/15836263/.

[25] Tsao, Tzeta & Slamani, Mustapha & Varshney, P.K. & Weiner, D. & Schwarzlander, H. & Borek, S.. (1997). Ambiguity Function for a Bistatic Radar. Aerospace and Electronic Systems, IEEE Transactions on. 33. 1041 - 1051. 10.1109/7.599331.

[26] "Electronic Code of Federal Regulations." *ECFR*, ecfr.federalregister.gov/.

[27] "Makers of MATLAB and Simulink." *MathWorks*, www.mathworks.com/.

[28] Shampine, L.F. "Solving Delay Differential Equations with dde23." *Radford.edu*, www.radford.edu/~thompson/webddes/tutorial.pdf.

[29] *Linear Systems and Signals,* B.P. Lathi, electronicsbookcafe.files.wordpress.com/2015/08/Linear-Systems-and-Signals-2nd-edition-B-P-Lathi.pdf.